

FINAL REPORT

**Circulation and Cross-Shelf Transport and Exchange
Along the Bering Sea Continental Shelf Edge**

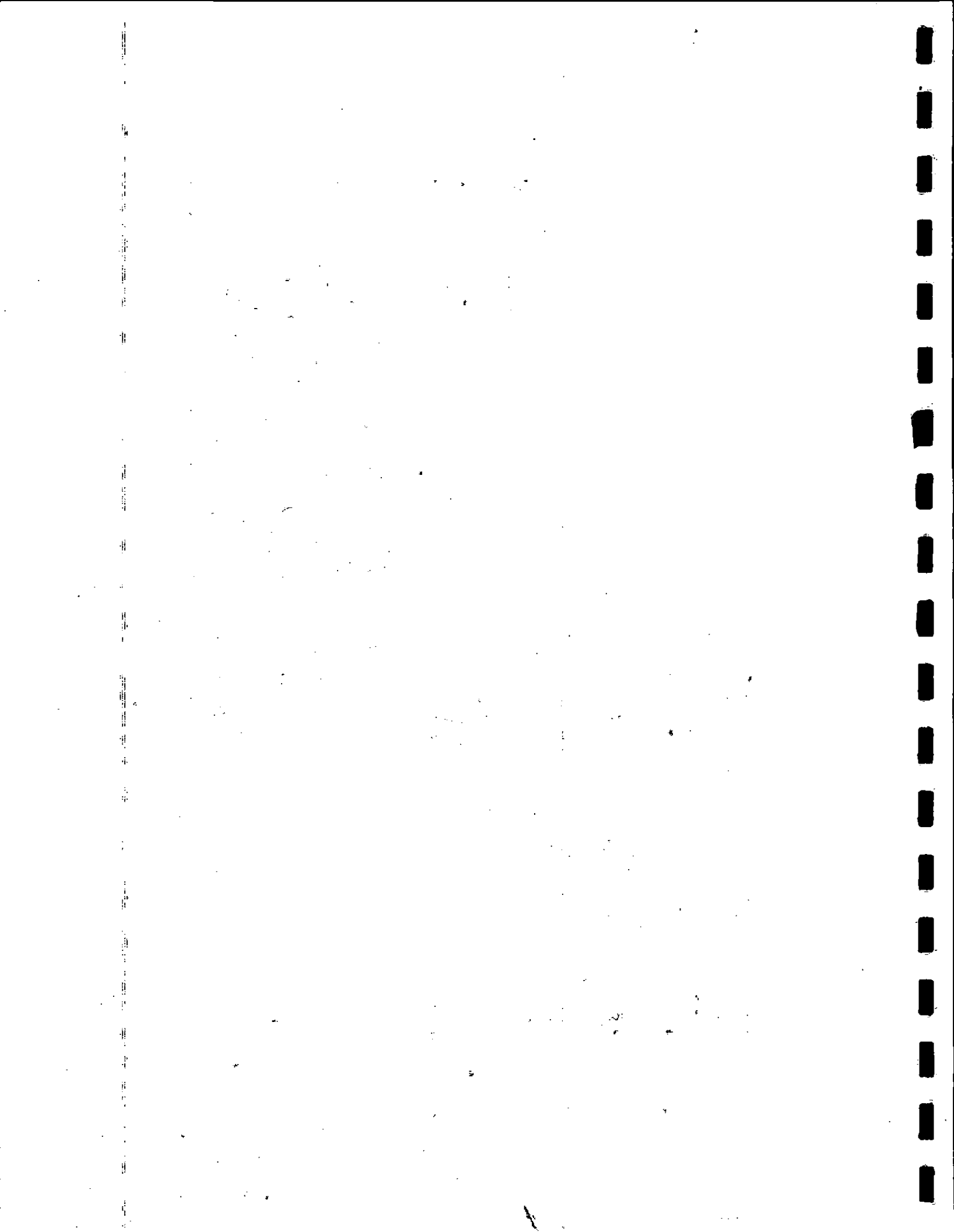
J. D. Schumacher and R. K. Reed

U. S. Department of Commerce
National Oceanic and Atmospheric Administration
Pacific Marine Environmental Laboratory
7600 Sand Point Way N.E.
Seattle, Washington 98115

This study was funded in part by the Alaska Outer Continental Shelf Region of the Minerals Management Service, U.S. Department of the Interior, Anchorage, Alaska through Inter-agency Agreement 14-35-0001-14165 with the Pacific Marine Environmental Laboratory, National Oceanic and Atmospheric Administration, U.S. Department of Commerce.

June 1993

The opinions and findings here are the authors' and do not necessarily reflect those of the U.S. Department of the Interior, nor is mention of trade names an endorsement.

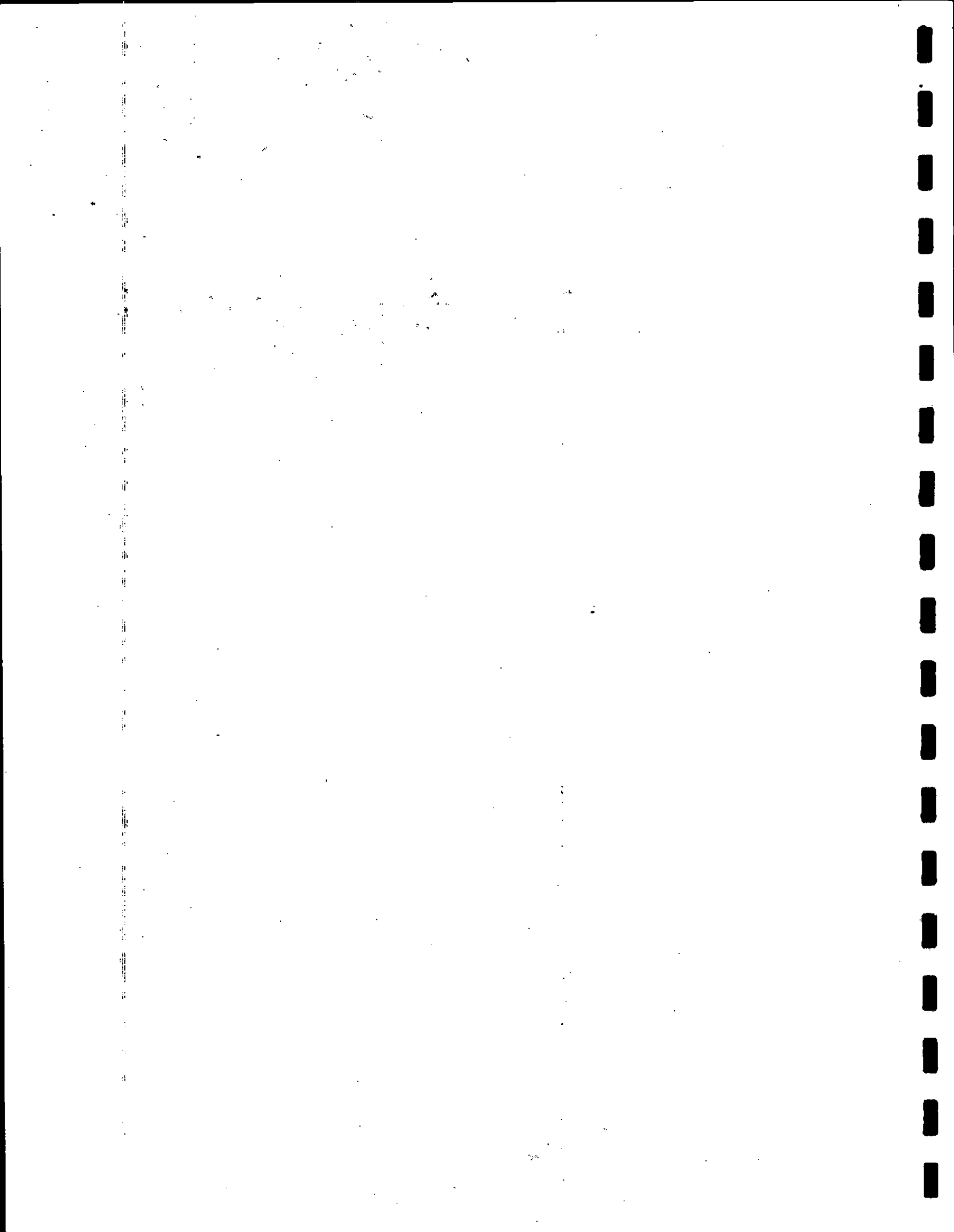


OCS Study MMS 93-0027

**Circulation and Cross-Shelf Transport and Exchange
Along the Bering Sea Continental Shelf Edge**

J. D. Schumacher and R. K. Reed

U. S. Department of Commerce
National Oceanic and Atmospheric Administration
Pacific Marine Environmental Laboratory
7600 Sand Point Way N.E.
Seattle, Washington 98115



CONTENTS

	PAGE
ABSTRACT	1
INTRODUCTION	2
DATA AND METHODS	4
RESULTS	6
Geostrophic Flow	6
Physical Property Distributions	6
Horizontal Distributions of Surface Salinity	6
Vertical Sections of Temperature and Salinity	6
Temperature Near the Subsurface Maximum	10
Nutrient Distributions	10
Vertical Sections of Nutrients	10
Nutrients at 100 db	13
Measured Currents	13
Mean Currents	13
Low-Frequency Currents	13
Eddy Kinetic Energy	20
Spectral Estimates	20
Fluxes of Momentum, Heat and Salt	20
Results of Drifter Trajectories, 1989-1990	22
10 September 1989 Deployment	22
23 September 1989 Deployment	22
19 April 1990 Deployment	25
1 May 1990 Deployment	25

DISCUSSION	25
ACKNOWLEDGMENTS	29
REFERENCES	30
LIST OF TABLES	32
APPENDIX I	37
APPENDIX II	38

ABSTRACT

Data from three CTD (conductivity, temperature, depth) surveys conducted during Outer Continental Shelf Environmental Assessment Program (OCSEAP) cruises in the central Bering Sea during fall 1989, spring 1990, and fall 1990 are used to examine circulation and property distributions. Geostrophic flow was quite variable, except in Pribilof and Zhemchug Canyons where it was consistently westward. The variability of flow and small transports are difficult to reconcile with any permanent current system. The relatively cold temperatures near the temperature maximum suggest the absence of inflow through Amukta Pass near 172°W. The distributions of nutrients in fall 1989 and spring 1990 are also presented and discussed. Small errors in the data, probably in silica, as a result of freezing the samples, precluded their use in detailed analyses.

Between September 1989 and October 1990, twenty-six current records were collected by instruments on eight moorings located in Pribilof and Zhemchug canyons, and at a site between these features. These records provide the first Eulerian measurements from the slope and mid-slope of the eastern Bering Sea. Results from the current observations, together with water property observations, permit a characterization of regional flow. There was a moderate flow (~2 to 18 cm/s) which followed the bathymetry toward the northwest. The flow was generally intensified in the upper 300 m. Wind and current energy increased in winter, but vector mean currents did not increase; only a small fraction of current fluctuations were coherent with wind forcing, however. The moorings were in the shoreward edge of the Bering Slope Current. At one mid-slope location in Pribilof Canyon, local bathymetry resulted in rectification of the strong daily tidal current. Small (5–30 km) eddies with strong (20–30 cm/s) rotational speeds were common features. Estimates of salt fluxes indicate significant shoreward flux; this, however, did not occur preferentially in the canyons.

Four sets of satellite-tracked drifting buoys were released at a site in the southeastern part of the area. One set released in fall 1989 met criteria for chaotic flow, but the other sets did not. The existence of chaos may be a factor in the variability and lack of permanence in the flow. There is also the suggestion of a seasonal change in circulation. The fall-winter data provided evidence for relatively strong westward flow, but spring-summer data suggested weak flow on the shelf.

INTRODUCTION

There are many schemes of mean circulation over the Aleutian Basin of the Bering Sea (e.g., Hughes et al., 1974; Sayles et al., 1979; Coachman, 1986). These depictions are based almost entirely on inferences from water properties. In all of the data sets used to map geopotential topography, station coverage was sparse and typically lacked synopticity. Common to all schemes is mesoscale variability exemplified by eddies (most prominent in the southeastern corner of the basin) and a band of northwesterly flow contiguous along some portion of the eastern boundary of the basin. In the vicinity of the continental slope, circulation seems to have characteristics (weak and variable) typical of eastern boundary currents.

Two oceanographic features are associated with the eastern continental slope: "a diffuse, large (nearly 1000 km long), and persistent (years) haline front" (Kinder and Coachman, 1978) and the Bering Slope Current (Kinder et al., 1975; Kinder, 1976; Kinder and Coachman, 1978; Kinder et al., 1986). The Bering Slope Current is described as a sequence of northwesterly, southeasterly, and northwesterly flowing bands with a net transport of -5×10^6 m³/s (Kinder et al., 1975). Until now, Eulerian measurements of currents over the slope were not available. Over the outer continental shelf, however, numerous direct measurements indicate a mean flow of 5 to 15 cm/s toward the northwest (Schumacher and Kinder, 1983; Muench and Schumacher, 1983).

The "Circulation and Cross-Shelf Transport and Exchange Along the Bering Sea and Continental Shelf Edge" study was conducted by personnel at the Pacific Marine Environmental Laboratory through sponsorship of the National Oceanic and Atmospheric Administration's Outer Continental Shelf Environmental Assessment Program (OCSEAP) and the Minerals Management Service (MMS). The objective of the study was to enhance understanding of water exchange and of property and momentum fluxes between the basin and shelf of the eastern Bering Sea. A major consideration was the effect of submarine canyons on exchange processes. Conductivity/temperature/depth (CTD) and nutrient data were collected during three OCSEAP cruises (September 1989, April–May 1990, and September–October 1990). Satellite-tracked drifting buoys were also deployed on the cruises.

Between September 1989 and October 1990, eight moorings recorded data near the continental slope of the eastern Bering Sea (Fig. 1). The resulting current time series provide the first opportunity to describe the velocity field using long-term moored observations. A major goal was examining the possibility of regional differences in the flux of water properties from the slope to the shelf. Previous results from water property and nutrient data suggested that both Pribilof and Zhemchug Canyon acted as conduits for transport onto the shelf (Kinder, 1976). Distributions of total suspended matter collected in the vicinity of Zhemchug Canyon suggested that superimposed on the northwesterly drift are both eddies and a cross-shelf component of flow (Karl and Carlson, 1987). Also, high primary production over the northern Bering Sea shelf is likely supported by nutrients which are transported from the Bering Slope Current onto the shelf (Hansell et al., 1989). With this knowledge, we designed an array of moorings which included moorings in Zhemchug and Pribilof Canyon and along a "straight" section of the slope located between the canyons.

We first present results from the water property data to infer circulation. Analysis of direct current observations are then presented as mean and low frequency flow. The data are also examined for spectral properties and for fluxes of momentum, heat, and salt. Finally, we discuss results in the context of the previous understanding of the Bering Slope Current. In two appendices, we list published studies using these data and provide information on tidal current constituents.

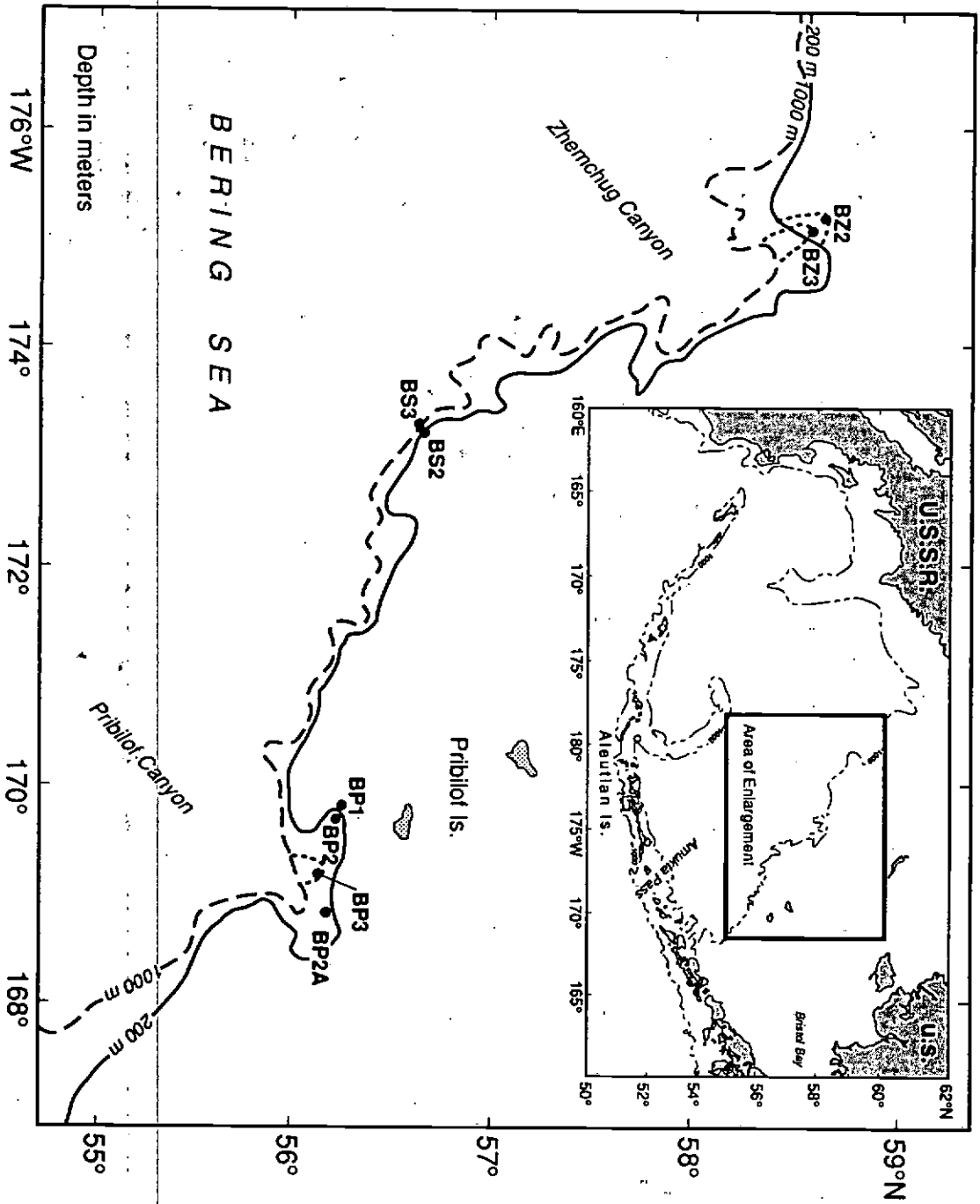


Figure 1. Study area showing the location of the current moorings. The general bathymetry is from standard NOAA/NOS charts. The dotted bathymetry is from ship soundings taken during operations and from Fischer et al. (1982). The insert shows the location of the eastern slope relative to the Bering Sea.

DATA AND METHODS

Essentially the same station grid was occupied on each of the three cruises in the study; the locations of the stations are shown in Fig. 2. CTD casts were taken during the cruises with a Seabird SBE-9 system to 1500 m or, in lesser depths, to within about 10 m of the bottom. Data were recorded (on disk in a minicomputer) only during the downcast at lowering rates of 30–50 m min⁻¹. Temperature and salinity corrections were derived from data taken on most casts. Various routines were used to eliminate spurious data and to derive 1-m averages of temperature and salinity, which were used to compute density and geopotential anomaly.

Nutrient samples were usually taken on alternate CTD casts at depths of 3, 10, 25, 50, 75, 100, 150, 200, and 300 m, and near bottom. Samples were drawn from Niskin bottles on the rosette sampler into 125-mL polyethylene bottles and were frozen for later analyses ashore. The analyses were performed on a Technicon Autoanalyzer II following methods of Whitledge et al. (1981). They yielded measurements of nitrate (NO₃), nitrite (NO₂), ammonia (NH₃), phosphate (PO₄), and silica (SiO₄).

During fall 1989 and spring 1990, eight moorings were deployed in the vicinity of the eastern Bering Sea slope (Figure 1). The plan was to deploy three arrays with moorings over the outer shelf (nominal depth 150 m), on the mid-slope (nominal depth 275 m), and on the slope (nominal depth 1000 m). The arrays were deployed in Pribilof and Zhemchug canyons and at a location between the canyons where the bathymetry was relatively linear. Due to mechanical problems with some of the acoustic releases, deployment of four moorings was delayed until the spring cruise in 1990. The position of one mooring was changed from the outer shelf at the central site to mid-slope (BP2A) in Pribilof Canyon. All moorings were either taut-wire or Kevlar line. The upper current meter was located at approximately 50 m below the surface and had a paddle wheel rotor to limit contamination of the desired signal by surface waves. The instruments were Aanderaa RCM-4 or -7 current meters. The current meters also measured temperature, pressure, and conductivity, from which salinity was computed. The time series of temperature and salinity were compared to CTD casts taken upon deployment, in spring, and upon recovery. The absolute values of temperature and salinity used here are believed accurate to 0.2°C and 0.3 ‰.

The current meters had 1-hr sampling intervals. All current records were first edited for time base problems and data spikes. Harmonic tide analyses on 29-d record segments were computed every 14.5 d to produce the tidal characteristics from the hourly data. To examine mean and low frequency characteristics, the current records were filtered using a cosine squared Lanczos filter with a half-power point of 35 h. This series was resampled at 6 hours and used to calculate correlations, rotary spectra, and coherence. Current vector plots and flux calculations used daily averages of the low-pass data. Surface winds were computed from the Fleet Numerical Oceanography Center surface atmospheric pressure grid. Geostrophic winds were interpolated to locations near the three array sites. To represent surface winds, the geostrophic winds were rotated 20° anti-clockwise and reduced in magnitude by 30%.

On the cruises during fall 1989 and spring 1990, two sets each of satellite-tracked drifters were released near 55.2° N, 167.8° W. (Five, four, seven, and six drifters were released during 10 September 1989, 23 September 1989, 19 April 1990, and 1 May 1990, respectively.) The drifters actually were released along a short southwest-northeast trending line at intervals of 1.0 km. Thus they should have been subject to very small-scale inhomogeneities in flow.

The drifters had tristar drogues centered at ~40 m, and they were deployed by crane from the ship. Typically 15–18 position fixes were received per day through the Argos location system. One drifter was picked up by a fishing vessel 71 days after release and remained

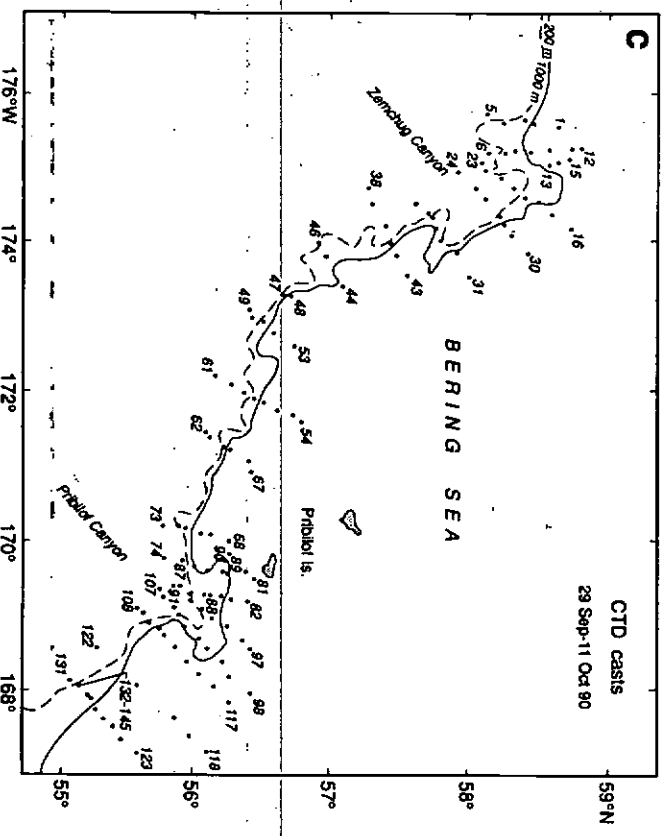
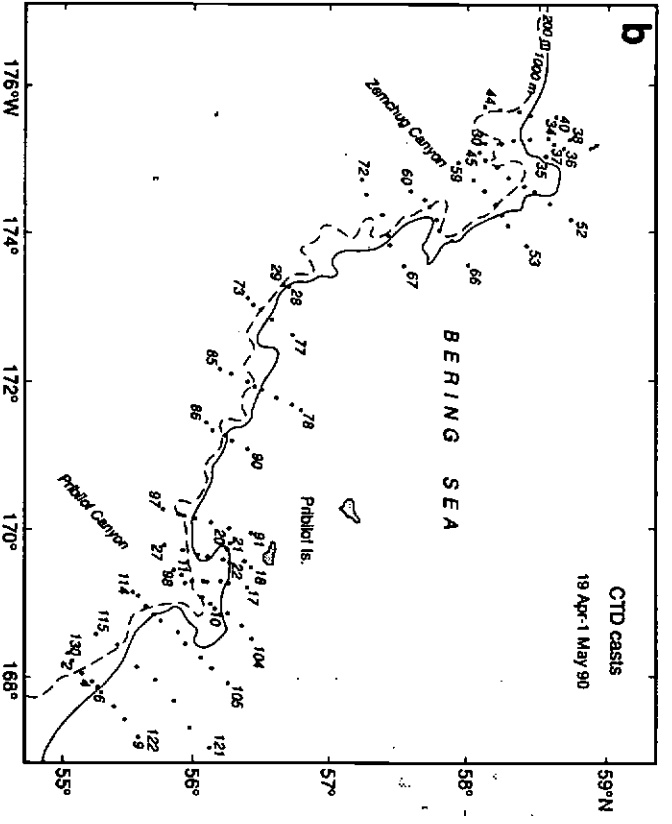
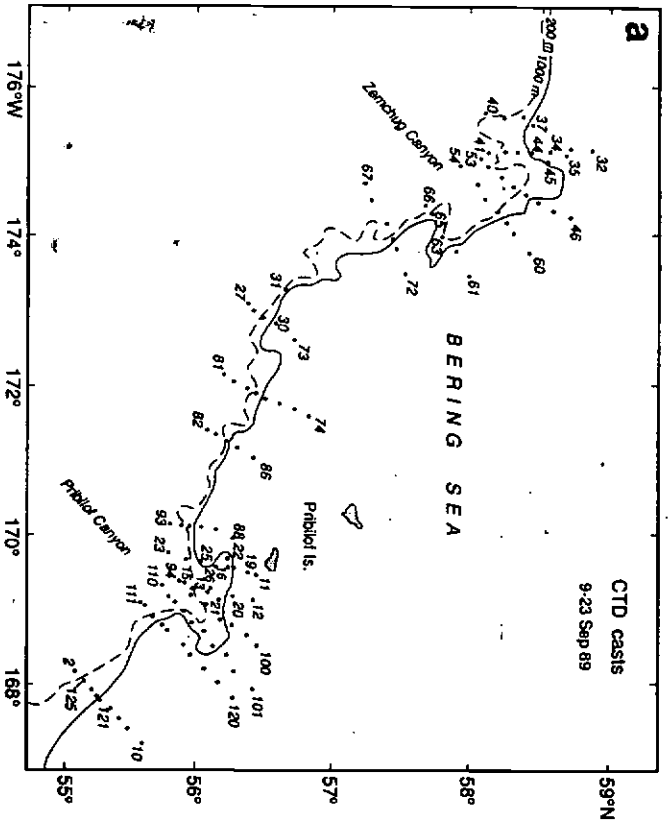


Figure 2. Locations of CTD castis taken in the central Bering Sea: (a) 9-23 September 1989, (b) 19 April-1 May 1990, and (c) 29 September-11 October 1990

stationary in port for 40 days; its standard error of position from the satellite system was only 0.18 km. In general, there were significant losses of data from our area of interest after 100 days. Hence only the initial 100 days of data results are shown and discussed here.

RESULTS

Geostrophic Flow

Although CTD casts were taken to a maximum depth of 1500 m, more data are available to infer circulation if a shallower reference level is used. Earlier work (Kinder et al., 1975; Reed et al., 1988; Reed and Stabeno, 1989) in this region suggests that 1000 m is a realistic reference level for upper-ocean geostrophic flow. The geopotential topography of the sea surface, referred to 1000 decibars (db; 1 db \approx 0.98 m), for the three cruises is shown in Fig. 3.

During fall 1989 (Fig. 3a), geostrophic flow in the southern part of the region and in Pribilof Canyon was to the northwest or west. Between $\sim 171^\circ$ and 175° W, however, flow was mainly to the southeast. Farther north (in Zemchug Canyon) flow was again to the northwest. In spring 1990 (Fig. 3b), a well-developed onshore flow was present in the southern part of the area. (At the start of this cruise, 19 April, the flow had been to the northwest, however.) Westward flow occurred in Pribilof Canyon, and northwestward flow occurred near Zemchug Canyon. In between the canyons, flow was southeastward or alternated between onshore and offshore. In fall 1990 (Fig. 3c), westward flow occurred in the canyons, although it was relatively weak. Between the canyons, regions of weak onshore or offshore flow were present. In summary, over this 1-year period there was considerable variability in flow along most of the slope.

At the start and end of both the fall 1989 and the spring 1990 cruises, satellite-tracked drifters were launched between stations 5 and 6 (Figs. 1a and 1b). The initial movements of the drifters were in good agreement with geostrophic flow estimates in all cases. Furthermore, flow along the slope was similar regardless of the reference level used. A 26-h time series of CTD casts was taken during 10–11 October 1990 (stations 132–145; Fig. 1c); the standard deviation of geopotential anomaly (0/1000 db) was only 0.007 dyn m, which suggests that internal tides had little effect on the geopotential topography. Thus the flows shown in Fig. 3 certainly appear to be realistic, and aspects of flow variability are discussed further.

Physical Property Distributions

Horizontal Distributions of Surface Salinity. Sea-surface salinity in this area has large spatial and temporal variability, especially over the shelf (Reed et al., 1988; Reed and Stabeno, 1989). The distributions shown in Fig. 4 reflect the effects of freshwater discharge, ice formation, and mixing. They also are similar to the distributions of surface flow over the shelf, referred to a shallow level such as 100 db (not shown).

The patterns shown in Fig. 4 do not vary greatly during the three periods. Salinity $< 32.0\text{‰}$ was found during each cruise near the Pribilof Islands. This is an extension of the low-salinity water from outer Bristol Bay (Schumacher and Kinder, 1983). Shelf water elsewhere was typically 32.2–32.6‰. There was considerable variability in the surface salinity of the offshore waters, but values of 32.4–32.8‰ were common. The patterns suggest weak northwest flow over most of the shelf. Offshore, the distributions should not be used to infer surface flow because the deeper baroclinic structure is quite important.

Vertical Sections of Temperature and Salinity. Figure 5 presents vertical sections of temperature and salinity for fall 1989 (stations 74–81) and spring 1990 (stations 78–85); these

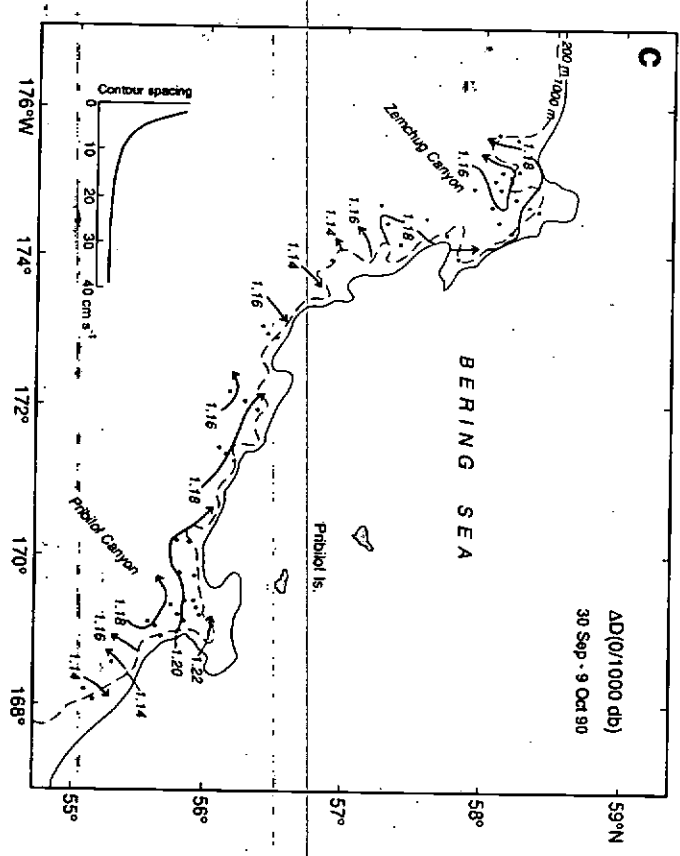
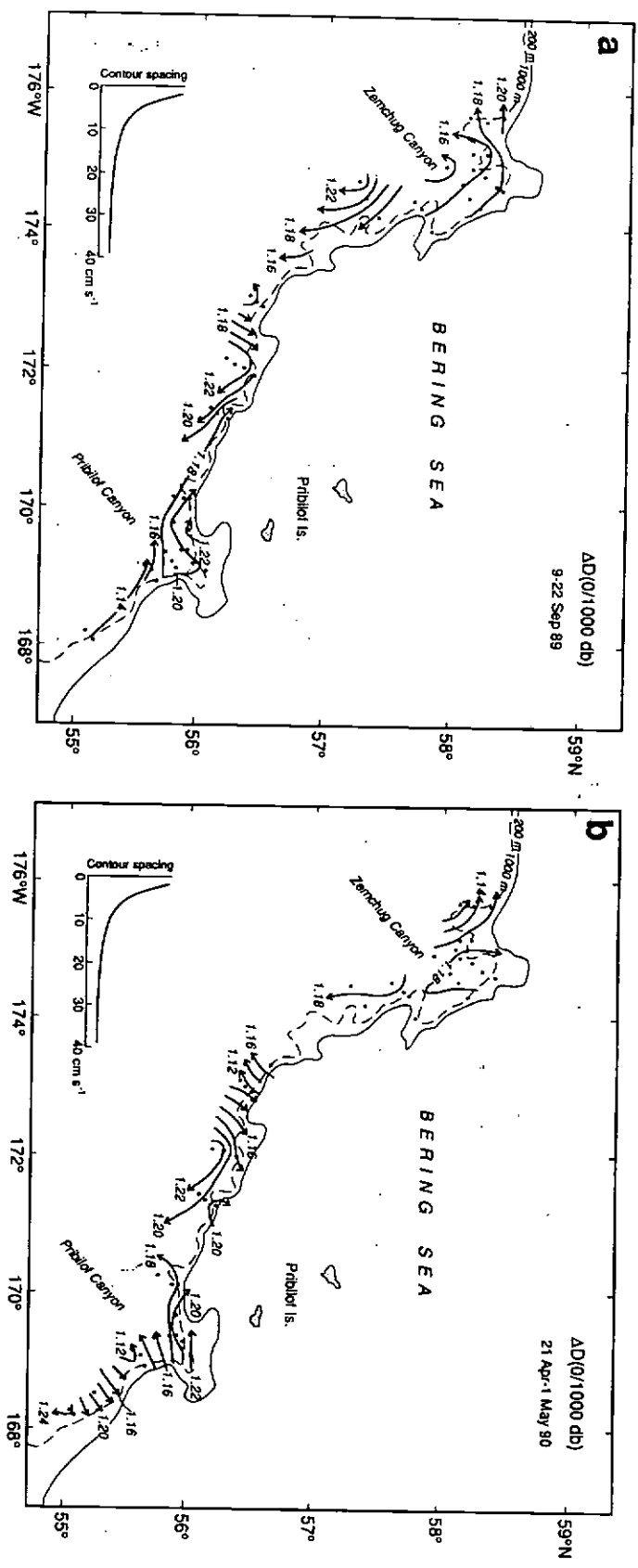


Figure 3. Geopotential topography (AD, dyn m) of the sea surface, referred to 1000 db: (a) 9-22 September 1989, (b) 21 April-1 May 1990, and (c) 30 September-9 October 1990.

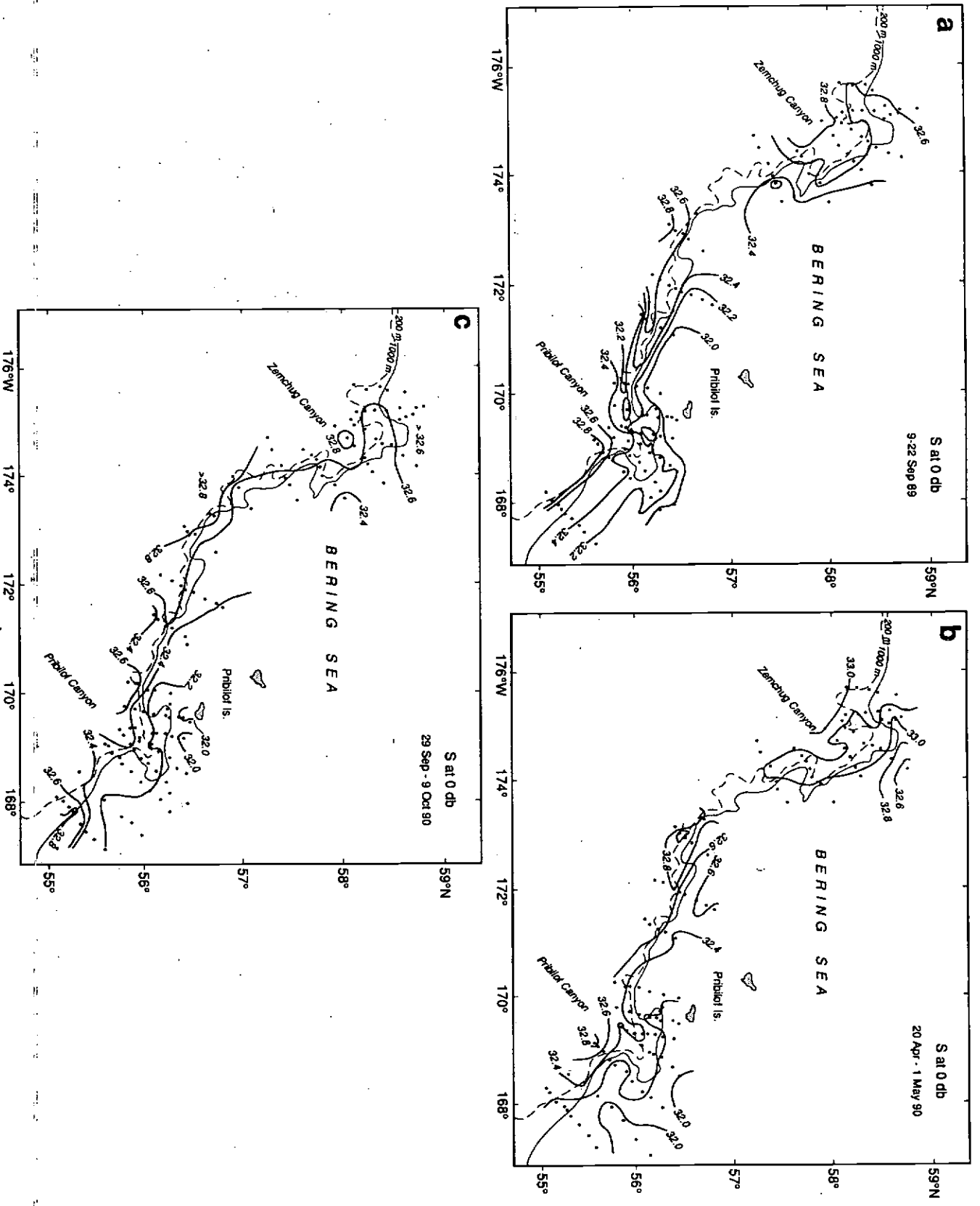


Figure 4. Horizontal distributions of sea surface salinity (‰): (a) 9-22 September 1989, (b) 20 April-1 May 1990, and (c) 29 September-9 October 1990.

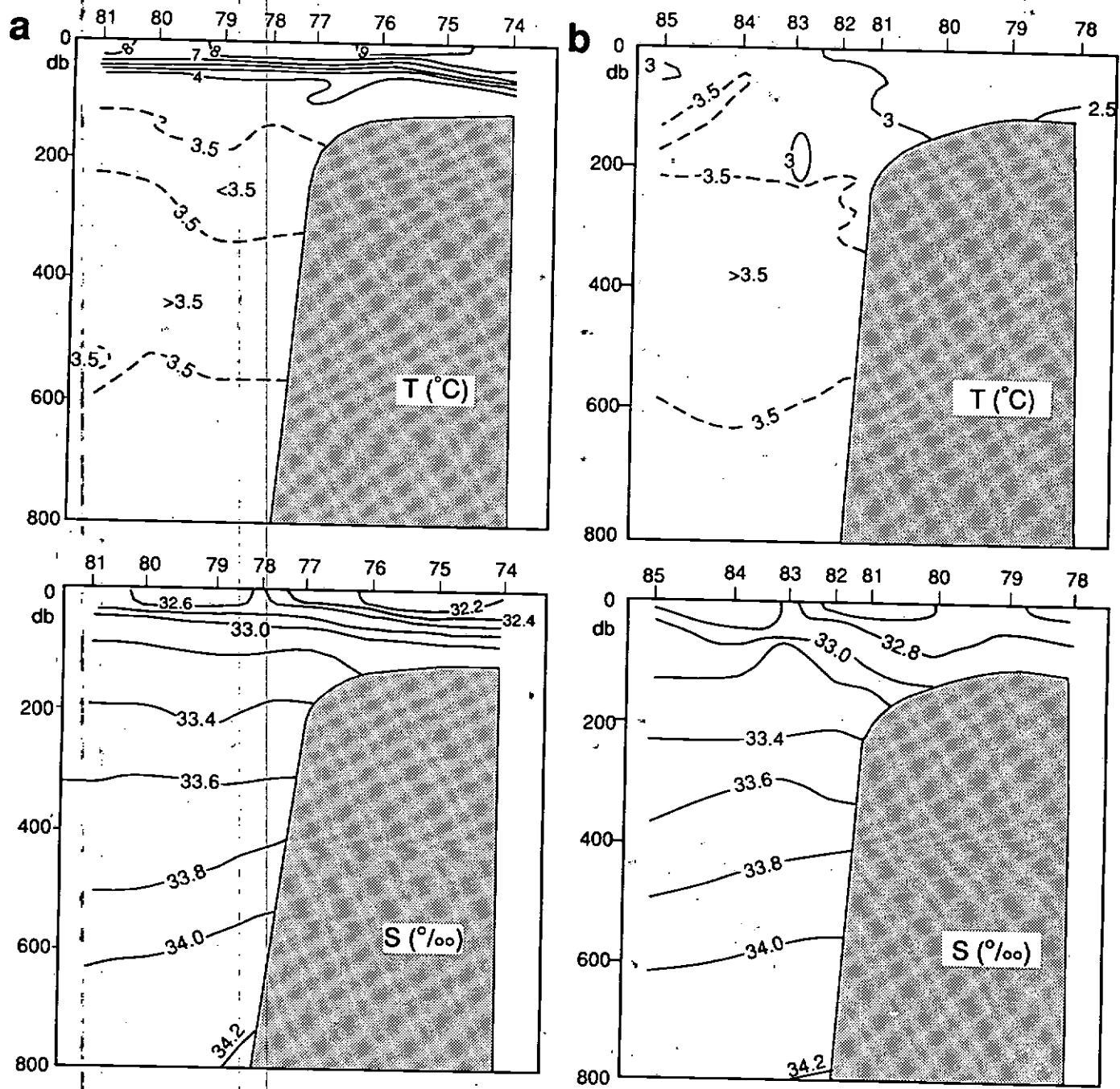


Figure 5. Vertical sections of temperature ($^{\circ}\text{C}$) and salinity (‰): (a) 19 September 1989 (stations 74-81) and (b) 27 April 1990 (stations 78-85).

data are from the same location over the slope and shelf near 172°W. These sections are also used to present nutrient data. Figure 5a shows surface temperatures of 7°–9°C. A subsurface temperature minimum (<3.5°C) was present near 200 db; a subsurface maximum (>3.5°C) was present near 400 db. In spring 1990 (Fig. 5b), surface temperature was near 3°C; the subsurface minimum was at the surface at some stations but below the surface at others. The maximum (>3.5°C) was again present near 400 db. The slope of the isohalines below ~200 db indicates southeast flow in agreement with Fig. 3. Surface salinity over the shelf was appreciably lower in fall 1989 (Fig. 5a) than in spring 1990 (Fig. 5b).

Temperature Near the Subsurface Maximum. The Bering Sea is characterized by a temperature-minimum layer, from the surface to near 200 db, and by a temperature-maximum layer below the minimum, typically centered at 300–400 db. The temperature minimum is deepest and has the most extreme (coldest) temperatures off the coast of Siberia and Kamchatka (Sayles et al., 1979); although it is formed by winter convection, it persists year-round, and its distribution is altered by subsurface advection and diffusion. On the other hand, the temperature-maximum layer is mainly affected by horizontal advection of water from the North Pacific through the Aleutian Island passes (Sayles et al., 1979). Kinder et al. (1975) concluded that the maximum occurred near the sigma-t density surface of 26.8, but Reed and Stabeno (1989) found the maximum occurred just south of the Pribilof Islands in spring 1988 at a mean sigma-t density of 26.62. Thus the depth and density of the maximum can vary considerably, presumably as a result of variations in the source waters.

Temperature near the maximum during the three OCSEAP cruises is shown in Fig. 6. The mean sigma-t densities at the maximum were 26.80 ± 0.09 , 26.76 ± 0.06 , and 26.78 ± 0.07 during fall 1989, spring 1990, and fall 1990, respectively. The mean temperatures on these surfaces were $3.65^\circ \pm 0.06^\circ$, $3.70^\circ \pm 0.06^\circ$, and $3.66^\circ \pm 0.04^\circ$ during fall 1989, spring 1990, and fall 1990, respectively. The mean differences are not statistically significant. In fall 1989 (Fig. 6a), the coldest temperatures were in the northern part of Pribilof Canyon, and the warmest were in Zemchug Canyon. The warmest temperatures in spring 1990 (Fig. 6b) were in two zones of temperature $>3.7^\circ\text{C}$, one near 170°W in Pribilof Canyon and one in Zemchug Canyon. The coldest were near 173°W. In fall 1990 (Fig. 6c), the coldest temperatures were north of Zemchug Canyon, and the warmest were in the southern part of the study area. In general though, there was not a trend of decreasing temperature toward the north during the three cruises. The relatively cold temperatures present during all these cruises suggest there was an absence of warm (Alaskan Stream) inflow through the central Aleutian Island passes.

Nutrient Distributions

Vertical Sections of Nutrients. Vertical sections of PO_4 , NO_3 , and SiO_4 are shown during 19 September 1989 (Fig. 7a) and 27 April 1990 (Fig. 7b). These are the same sections used for temperature and salinity in Fig. 5. The nutrients near the surface have considerably lower concentrations in fall 1989 than in spring 1990. The 1989 spring bloom of diatoms (late April and May; Whitley et al., 1986) appears to be responsible for the nutrient depletion recorded in September 1989. The effects of the 1990 spring bloom would not yet be apparent in April 1990.

All dissolved constituents in this region are strongly affected by circulation (Coachman, 1986). The concentrations of PO_4 and NO_3 at 200–300 db near the continental slope were higher during fall 1989 (Fig. 7a) than during spring 1990, which might imply enhanced onshore movement in fall 1989; for SiO_4 , however, this pattern was reversed. This disagreement suggests that there may be small systematic errors in one or more nutrients, perhaps as a result of freezing the samples. According to Parsons et al. (1984), low values often occur for silica, in frozen samples, at concentrations $>50 \mu\text{M L}^{-1}$.

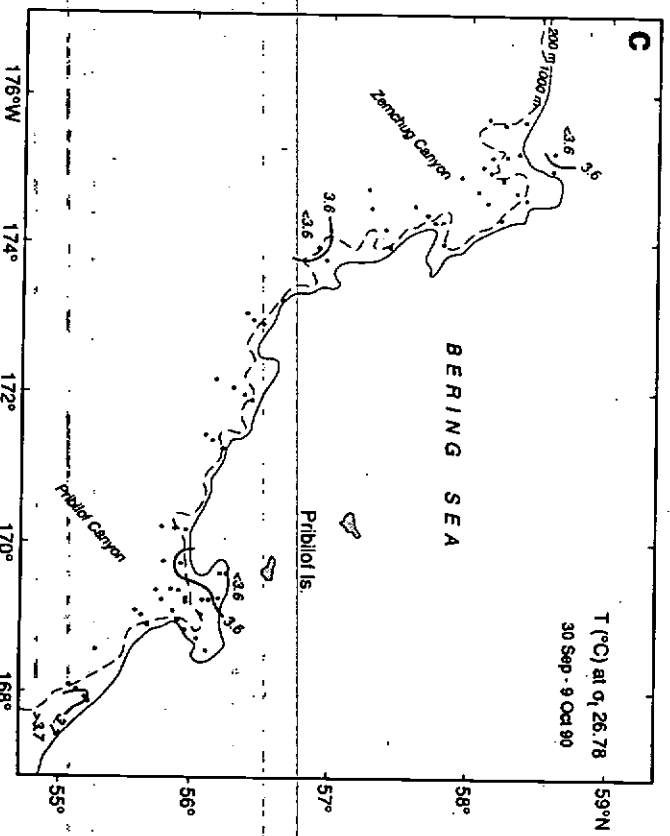
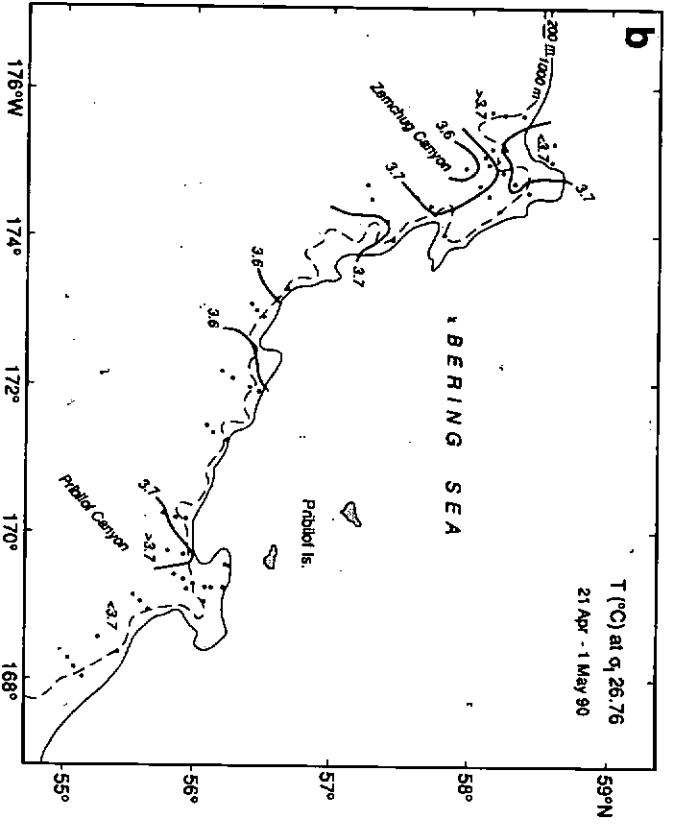
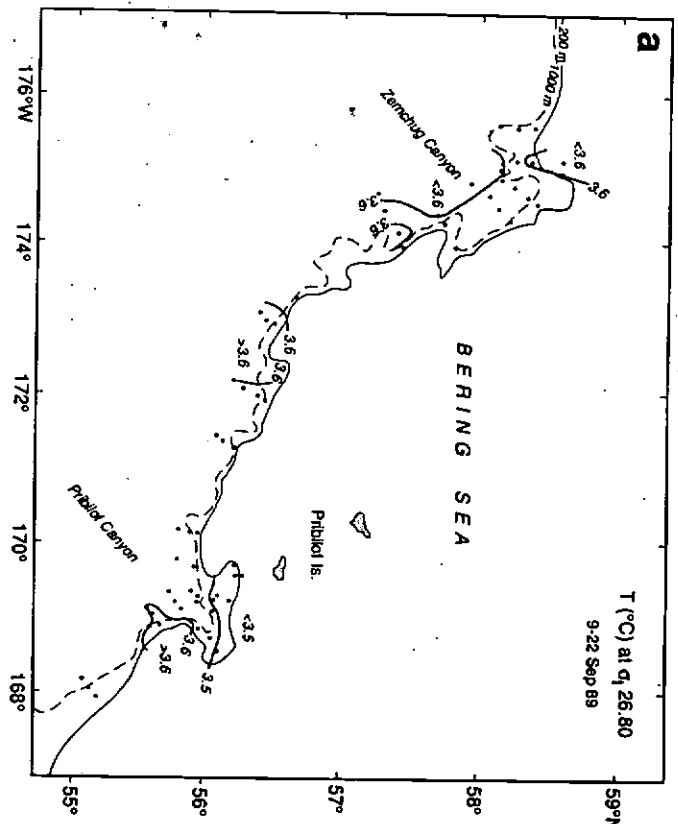


Figure 6. Distributions of temperature (°C) on the sigma-t density surface of (a) 26.80 (9-22 September 1989), (b) 26.76 (21 April-1 May 1990), and (c) 26.78 (30 September-9 October 1990).

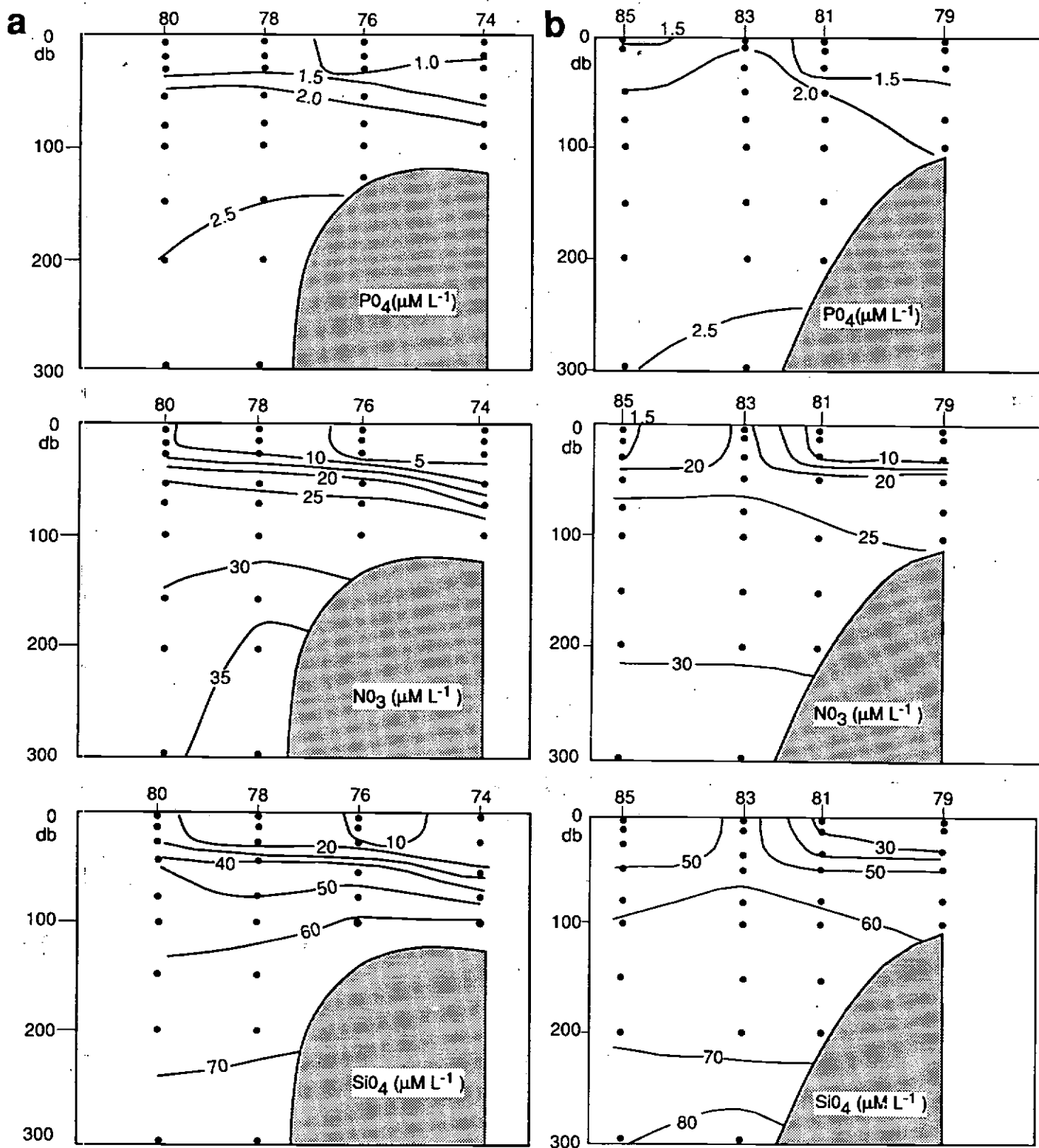


Figure 7. Vertical sections of phosphate (PO_4 , $\mu\text{M L}^{-1}$), nitrate (NO_3 , $\mu\text{M L}^{-1}$), and silica (SiO_4 , $\mu\text{M L}^{-1}$), (a) 19 September 1989 (stations 74–80) and (b) 27 April 1990 (stations 79–85).

Nutrients at 100 db. Concentrations of the three nutrients are shown for fall 1989 (Fig. 8) and spring 1990 (Fig. 9). The systematic differences discussed also appear in these figures. The patterns do not seem to reflect possible differences in origin of waters nor do they generally parallel the geostrophic flow. Much of the discrepancy would be removed, however, if the silica data for fall 1989 were systematically too low as a result of freezing of the samples.

Measured Currents

Mean Currents. All of the current records from locations in Pribilof Canyon have statistically significant vector mean flow (Table 1). In general the direction of flow was aligned with the large-scale bathymetry and was generally toward the west or southwest. This supports observations from the adjacent outer continental shelf (Schumacher and Kinder, 1983; Coachman, 1986) and is consistent with general inferences made from geostrophic estimates. At BP3, BP2A, and especially at BP2, the mean velocity was greater at the lowest level than at the observation level above it. Where the slope is relatively straight (BS2 and BS3), mean currents were strong and toward the northwest. It seems possible that the current was enhanced by the slope; mean flow at intermediate depths at BS2 was markedly greater than at similar depths at BS3. Mean flow in Zhemchug Canyon was weak compared to flow elsewhere, but it was statistically different than zero in the upper 250 m of the water column. The vector mean currents support the concept of a moderate flow generally toward the west or northwest along a large segment of the eastern Bering Sea slope.

Low-Frequency Currents. In Pribilof Canyon, velocity was remarkably consistent in direction and showed little indication of seasonal change in magnitude over the mid-slope region (Fig. 10). Over the mid-slope at BP2, there appeared to be frequent modulations of current magnitude. At BP2A there were several clockwise rotations of current vectors which could represent the passage of eddies. Currents over the outer continental shelf (BP1; Fig. 11) had characteristics similar to the mid-slope currents. In contrast, currents over the slope (BP3; Fig. 11) were more variable in direction and magnitude. At BP3, near surface current fluctuations had correlations (all estimates of correlation are at zero lag) with those at the next two deepest levels of 0.65 and 0.37, but there was no significant correlation with the deepest fluctuations. At BP2, the correlations along the mean current axes of data at the upper meter with those at 137 m and 272 m were 0.76 and 0.28, respectively. At BP2A, only the two upper records had significant correlations (0.68). Over the outer continental shelf (BP1), fluctuations in the two current records were well correlated (0.64). Estimates of horizontal correlations between fluctuations at various moorings indicated no significant values for most record pairs, except between the upper meters at BP1 and BP2.

Currents at BS2 and BS3 (Fig. 12) were both steadier in direction and stronger than flow inferred from geostrophic estimates or from nearly all of the other measurements. There are, however, several reversals of current. In all of the records from this region the mean and principal axes were nearly parallel, and most of the fluctuating energy was contained in the principal axis component. Over both the slope and mid-slope, currents were well correlated throughout the water column. At BS3, correlations between the upper record and those at 120 m, 255 m, and 495 m were 0.97, 0.88, and 0.56, respectively. At BS2, correlations between adjacent pairs at the three depths were similar (0.93 and 0.79). Horizontal correlation between BS2 and BS3 (upper records) was 0.93.

Over the slope off Zhemchug Canyon (BZ3), current direction was quite variable (Figure 13). The difference between the directions of mean flow and the principal axis decreased from 60° at 50 m to 1° at 500 m. At BZ2, the difference between axes was smaller. Over the slope (BZ3), the correlations between adjacent meters was ~0.55. At BZ2, correlation between the two upper records was higher (0.65) than that at BZ3. Between the two lower records, however, the correlation was about the same as that over the slope. An estimate of horizontal

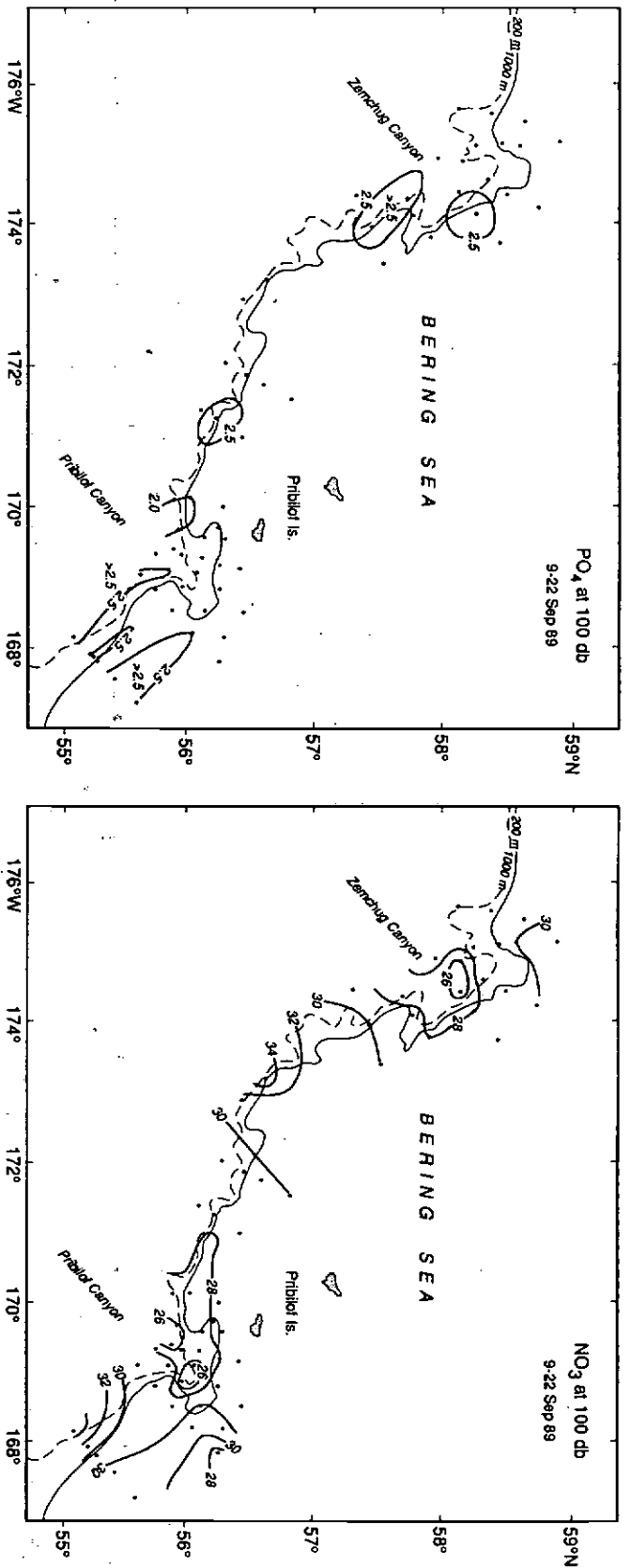


Figure 8. Horizontal distributions of (a) phosphate (PO₄, μM L⁻¹), (b) nitrate (NO₃, μM L⁻¹), and (c) silica (SiO₄, μM L⁻¹), at 100 db, 9-22 September 1989.

b

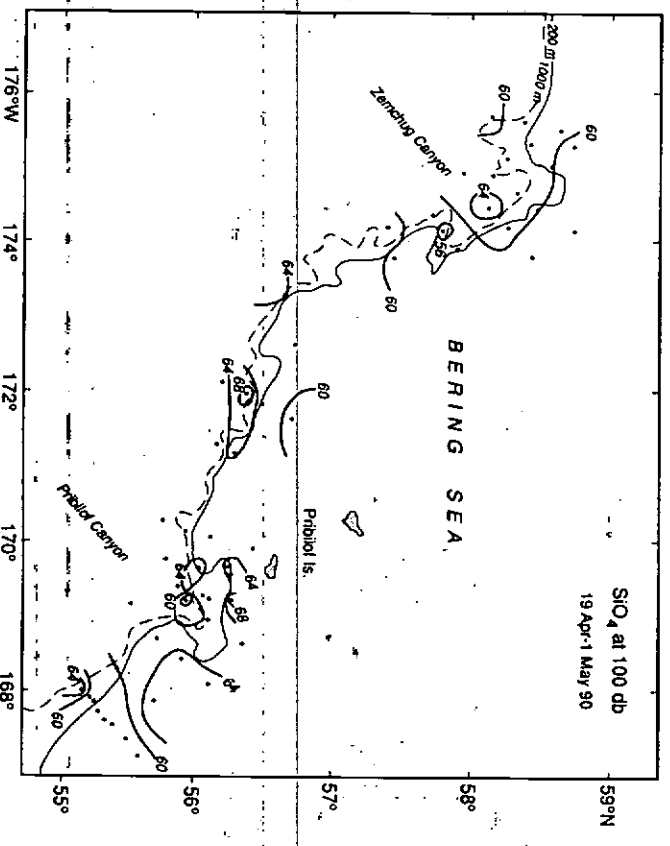
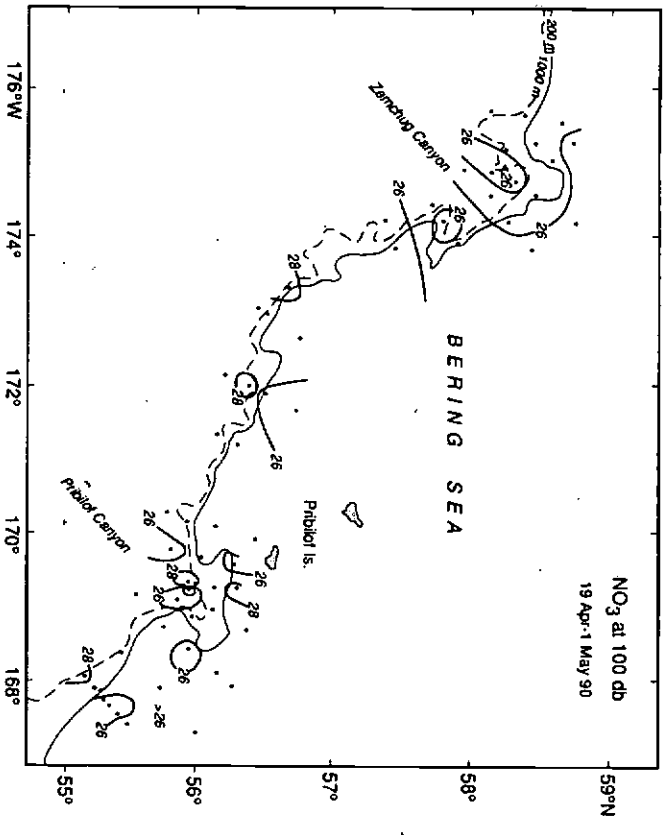
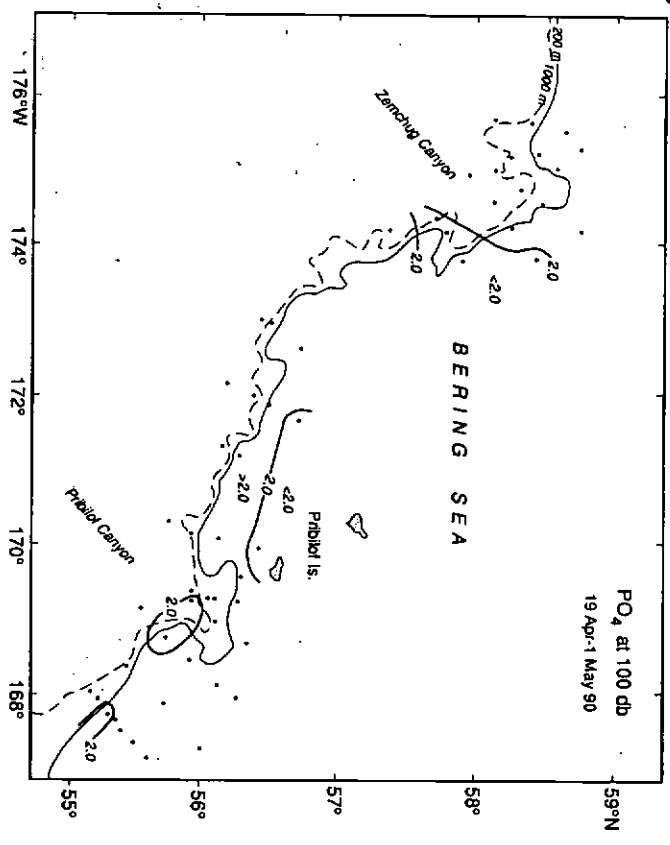


Figure 9. Horizontal distributions of (a) phosphate (PO_4 , $\mu\text{M L}^{-1}$), (b) nitrate (NO_3 , $\mu\text{M L}^{-1}$), and (c) silica (SiO_4 , $\mu\text{M L}^{-1}$) at 100 db, 19 April-1 May, 1990.

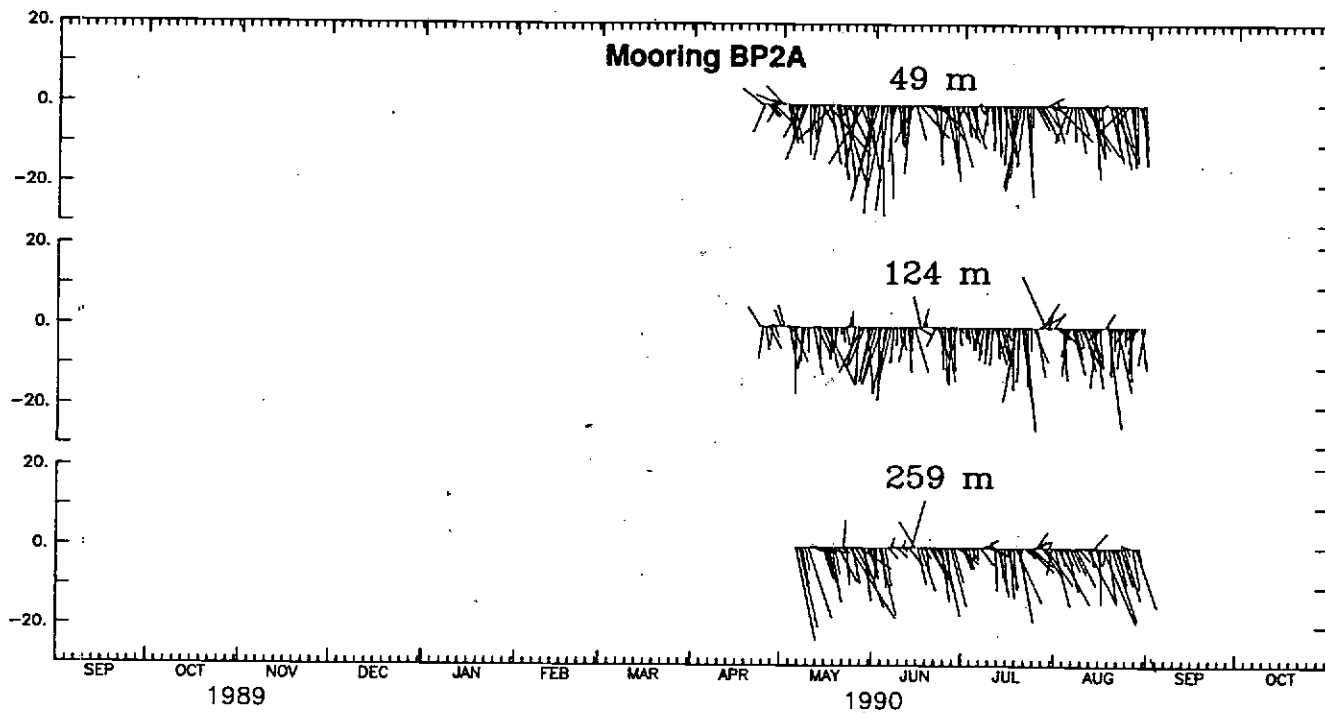
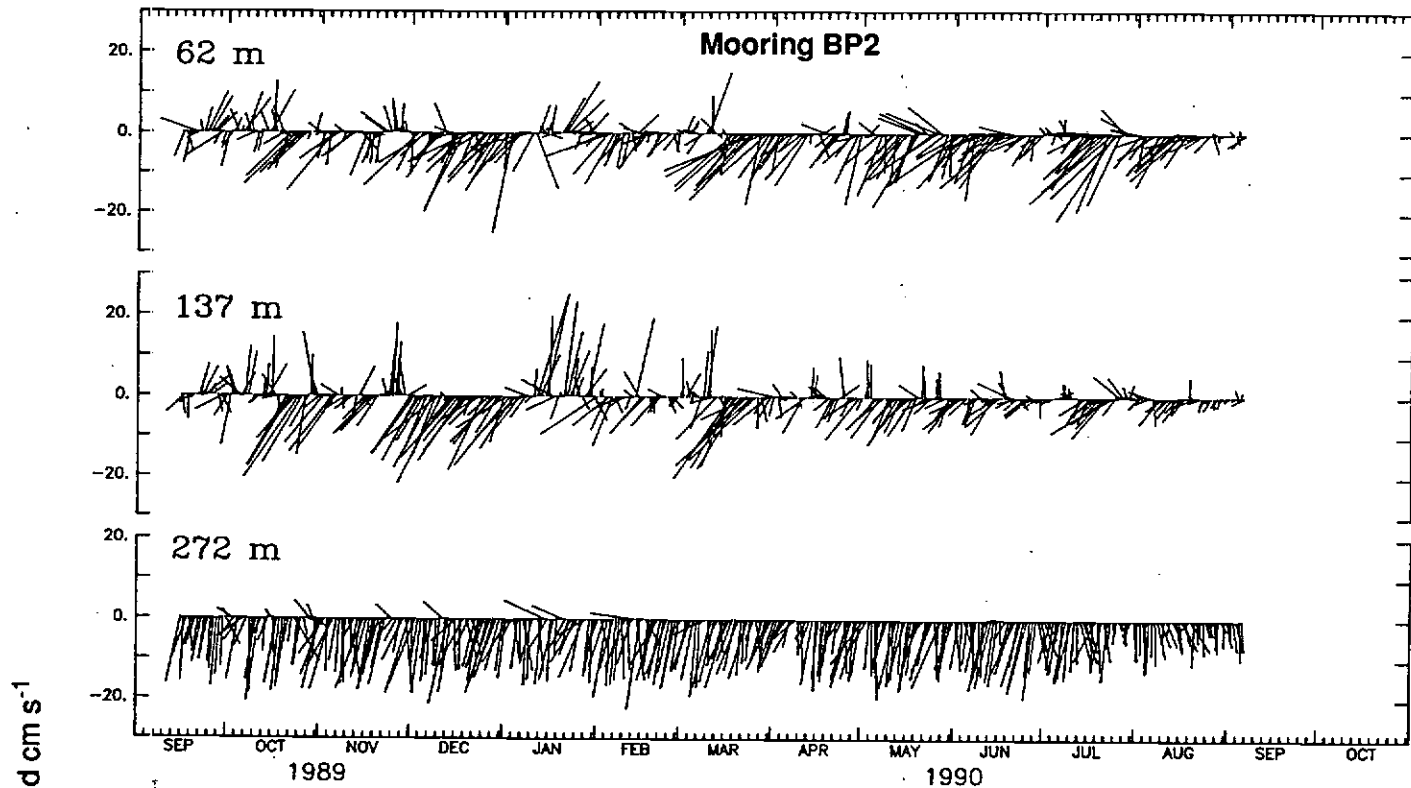


Figure 10. Daily averaged low-pass filtered currents over the mid-slope of Pribilof Canyon. Vectors from BP2 are in the upper panel and those from BP2A are shown in the lower panel (these vectors have been rotated 90° anti-clockwise so that they are not along the time axis; thus west is down). The vertical axes are speed in cm/s.

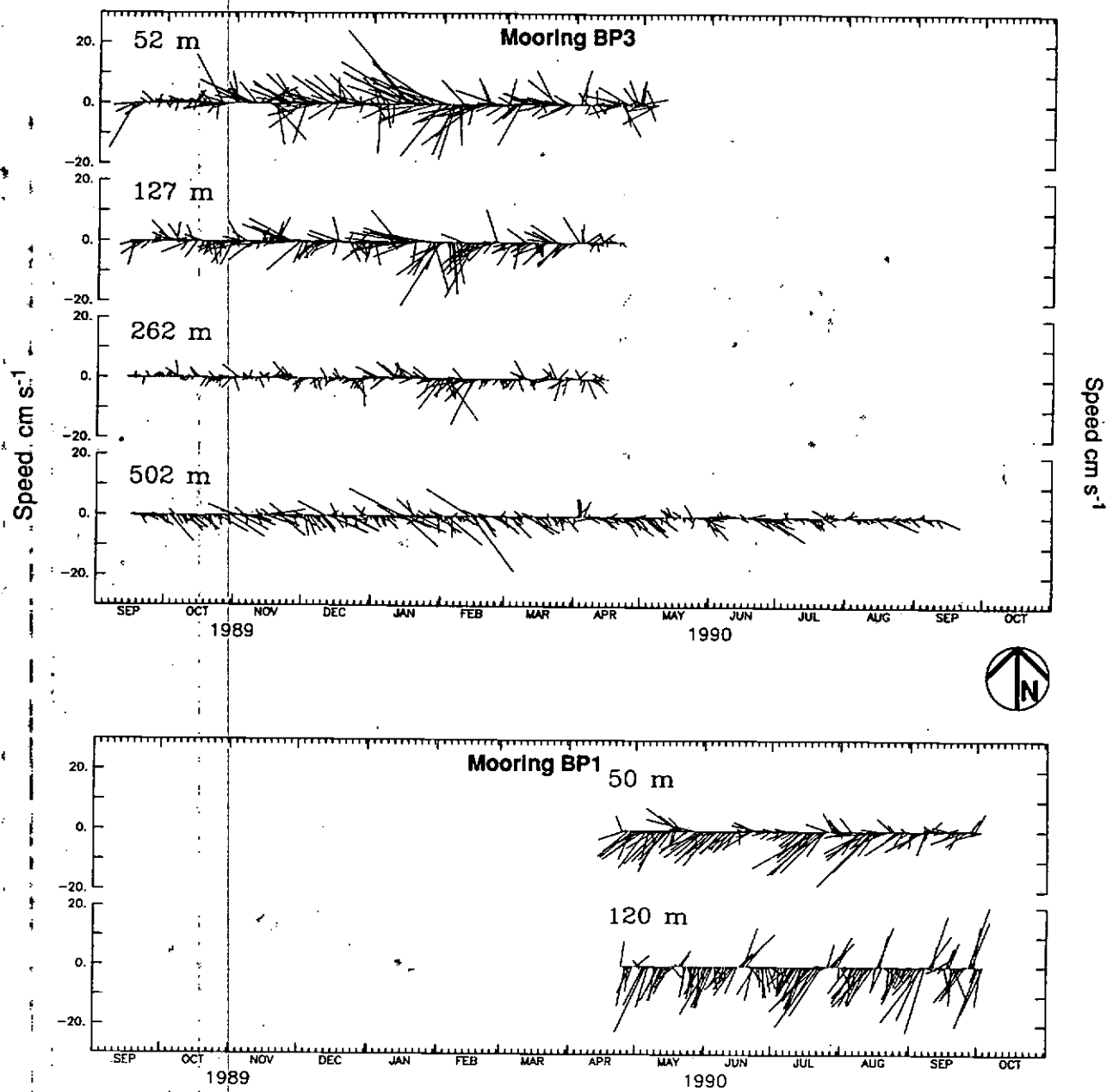


Figure 11. Daily averaged low-pass filtered currents over the slope (BP3) and outer continental shelf (BP1) in Pribilof Canyon. Up is north. The vertical axes are speed in cm/s.

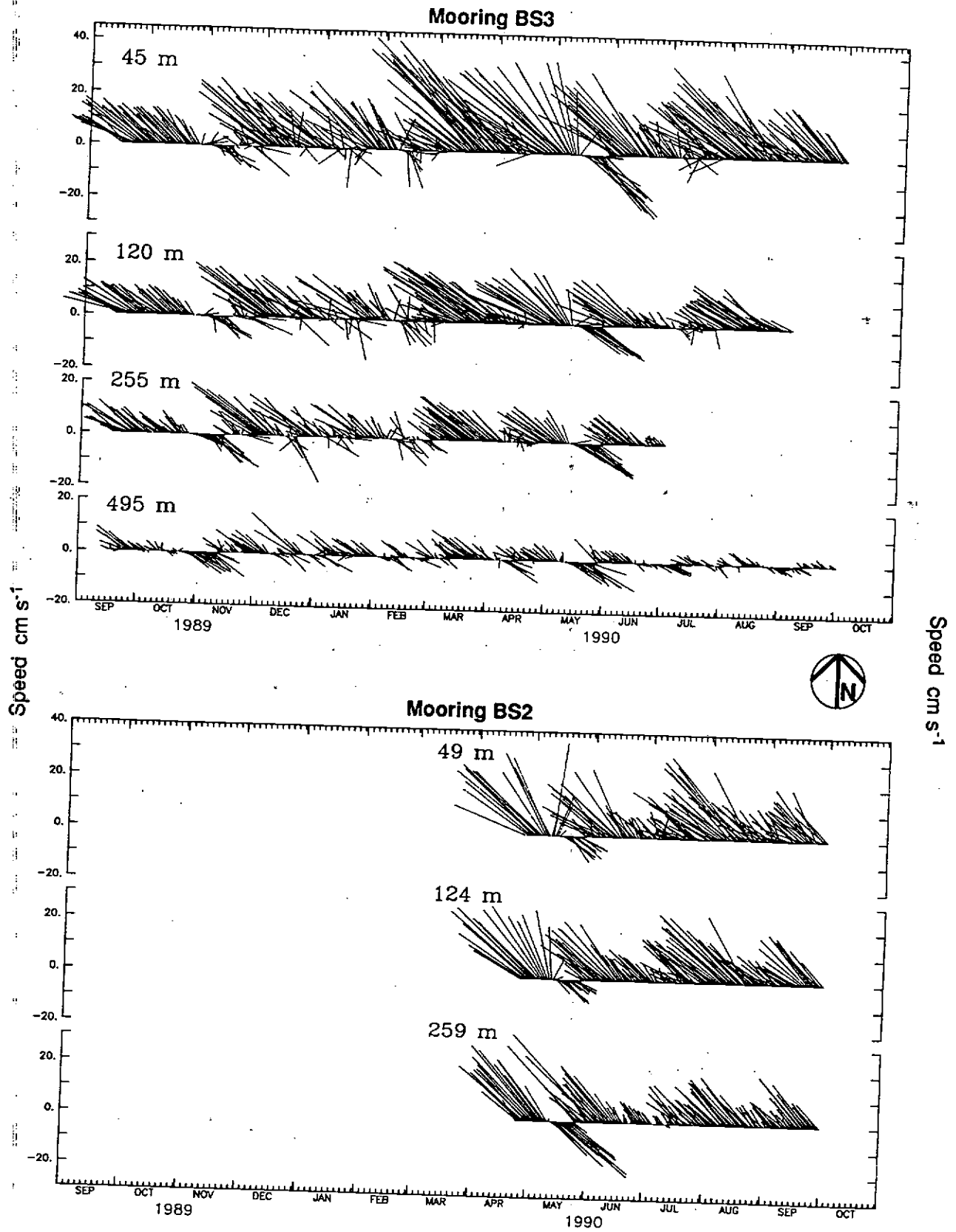


Figure 12. Daily averaged low-pass filtered currents over the slope (BS3) and mid-slope (BS2) at the central location. Up is north. The vertical axes are speed in cm/s.

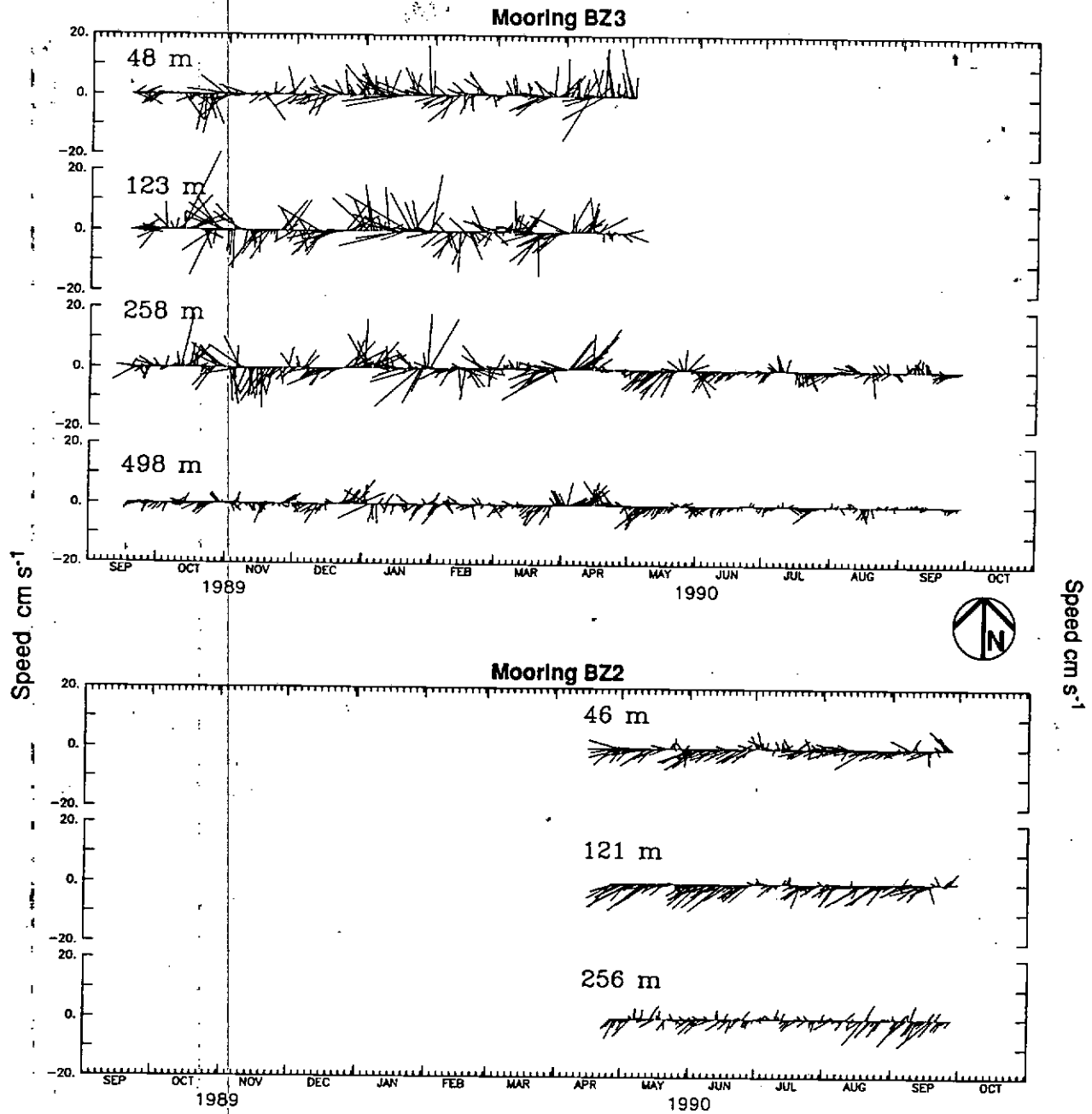


Figure 13. Daily averaged low-pass filtered currents over the slope (BZ3) and mid-slope (BZ2) in Zhemchug Canyon. Up is north. The vertical axes are speed in cm/s.

correlation between BZ2 and BZ3 (260 m and 258 m, the only simultaneous record pair) was 0.44.

Eddy Kinetic Energy. Estimates of subtidal eddy kinetic energy per unit mass (KE') were calculated from the along-and-across stream variances (Table 2). [The "summer" and "winter" seasons were previously defined using guidelines based on wind speed and variance of wind speed (Schumacher and Kinder, 1983)]. There appeared to be a seasonal signal in KE' for both current and wind, with winter being more energetic than in summer. Although in a given season wind energy was nearly uniform at all locations, eddy kinetic energy was lowest in Zhemchug Canyon. For the nine winter/summer current record pairs, three had larger vector mean flow in summer, and six had means that were not statistically different between winter and summer. This lack of seasonality in mean flow is consistent with results from the outer continental shelf (Schumacher and Kinder, 1983).

Spectral Estimates. There were marked maxima (13.9 d) in the spectra at all depths at BP2. In the near bottom record this maxima contained 17% of KE' . In addition, there were significant maxima (95% level of confidence) at other periods (between 2.5 and 9.0 d) in all the other current records. The amount of fluctuating kinetic energy in any of these, however, was <5% of the total.

In an attempt to account for the significant peaks in current spectra, linear and vector correlations between wind and current were estimated for all records. None of the correlation coefficients were significant, likely because much of the KE' in the currents was at periods >12 d. Estimates of coherence between current fluctuations along the mean axis and both parallel and orthogonal wind components did yield some significant (95% level) values that account for many of the observed maxima (in bands between 2.5 and 7.0 d). The total energy accounted for, however, was <10% of the total KE' . Interpreting results from coherence estimates is difficult, since the estimates are highly dependent on whether a record segment was winter or summer, and also on the length of record. Also, the geostrophic wind estimates are very crude. The strong maxima (13.9 d) at BP2 was not coherent with either wind component. Further analysis (Schumacher and Reed, 1992) showed that this strong near bottom net flow (Fig. 10) resulted from tidal rectification or enhancement of diurnal tidal motion into the net flow. This is shown in Fig. 14.

Fluxes of Momentum, Heat and Salt. One of the goals of this experiment was to ascertain the possible onshore transfer of momentum, heat, and salt across the shelf break. Furthermore, there was some thought that these fluxes might occur preferentially in the canyons rather than on the open slope. The computed values of the fluxes, performed on daily net velocity components and daily mean properties after use of a 35-hr filter, are listed in Table 3.

In general, the magnitudes of both the heat and salt fluxes are quite small. They are typically about half those measured at the shelf break in the Gulf of Alaska (Reed and Schumacher, 1986). Furthermore, most of them do not exceed their standard errors. Only 5, 5, and 5 of the fluxes $\overline{u'T'}$, $\overline{v'T'}$, and $\overline{v'S'}$, respectively, out of 26 possible, are significant; these percentages are somewhat less than would exceed one standard error by chance. On the other hand, 11 of the onshore salt fluxes ($\overline{u'S'}$) are significant, and all but one of these are positive. As expected, this indicates a flux of saltier waters toward the fresher waters inshore, unless there is negative eddy diffusivity or up-gradient flux. (Also, "diffusive" movement of our spring 1990 drifters near the BP moorings lend support to an onshore flux of materials.) It is interesting, however, that 5 of the significant fluxes occurred at the open-slope moorings (BS2 and BS3) and 5 were at the Pribilof Canyon sites. Thus there is no evidence that salt transfer occurs preferentially in the canyons, which had been one of our original hypotheses.

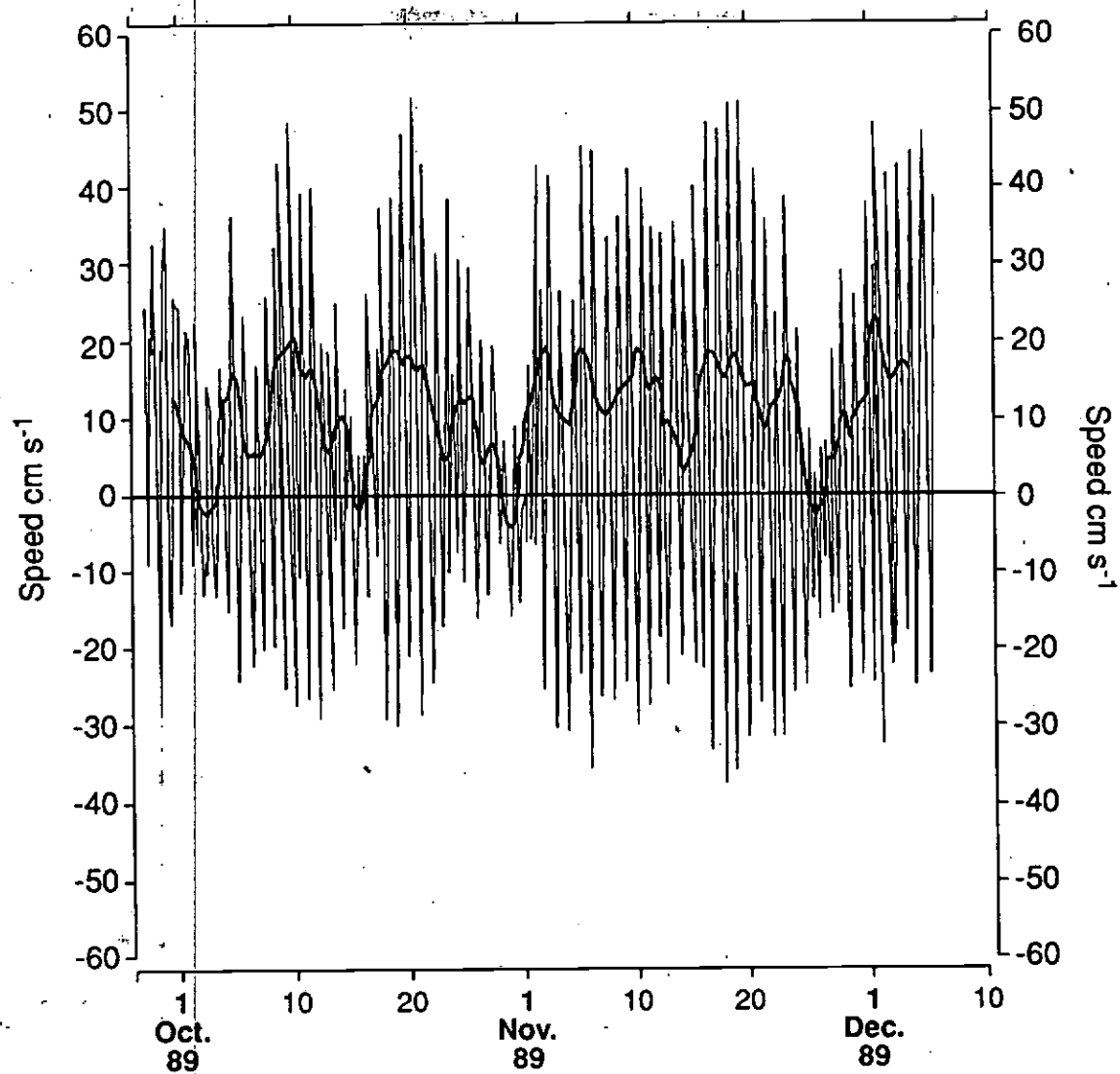


Figure 14. Segment of current data from BP2 (272 m). The tidal component (heavy line) is resolved on the principal axis (135°T) of the K1 constituent, and the low frequency component (vertical bars) is resolved on an axis of 185°T .

The momentum fluxes ($\overline{u'v'}$), however, tend to be more frequently significant and relatively larger than the property fluxes, except at moorings BZ2 and BZ3. Of the 19 remaining fluxes, 12 are significant; 4 out of 7 are significant at the open slope moorings (BS2 and BS3), and 8 out of 12 at the Pribilof Canyon sites.

At BS3 the significant $\overline{u'v'}$ values are negative; but the one significant value at BS2 is positive. Use of the relation, $-\overline{u'v'} = A_h \partial v / \partial x$, where A_h is the horizontal eddy viscosity and $\partial v / \partial x$ is the cross-stream gradient of alongstream flow, allows an estimate of eddy viscosity. Using a mean $\overline{u'v'}$ at BS3 of $-21 \text{ cm}^2 \text{ s}^{-2}$ (Table 3) and $\partial v / \partial x$ of $6 \text{ cm s}^{-1} / 3.3 \text{ km} = 1 \times 10^6 \text{ cm}^2 \text{ s}^{-1}$, which is a plausible, positive eddy viscosity. The significant positive $\overline{u'v'}$ at BS2 would require a decrease in velocity inshore, which seems likely, for the eddy viscosity to remain positive. There is a change in sign of $\overline{u'v'}$ between the upper and deeper meters at BP2 and BP1; the very small shear between these sites though makes an estimate of A_h , as above, meaningless.

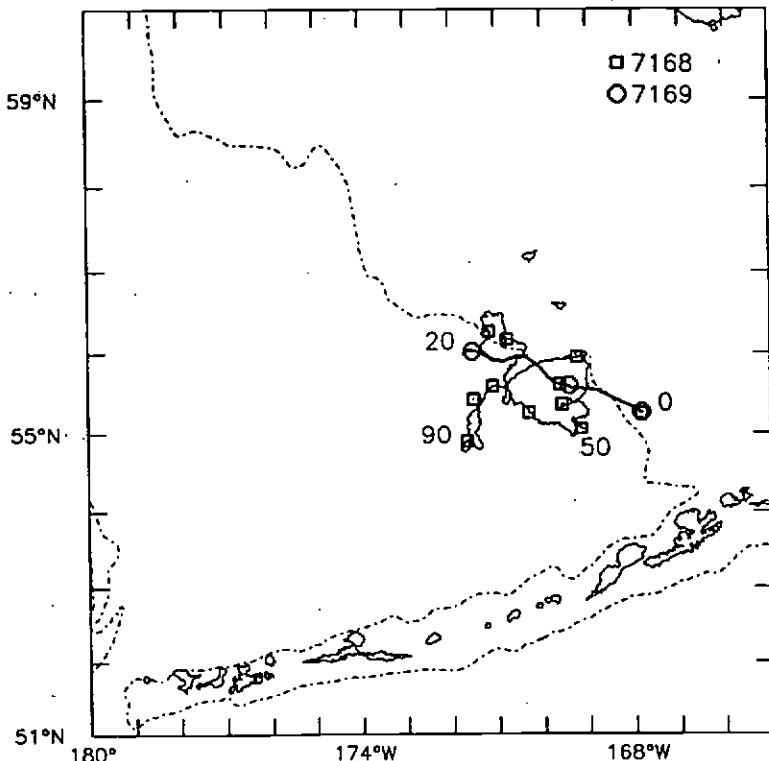
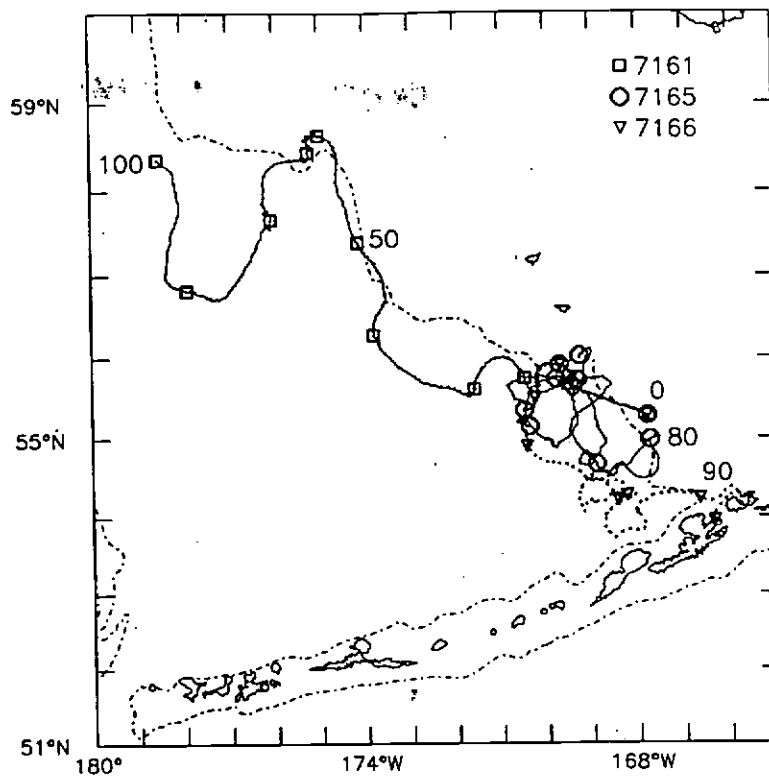
Results of Drifter Trajectories, 1989-1990

10 September 1989 Deployment. This set of five drifters initially moved westward across the 1000 m isobath (dotted line; Fig. 14) at a speed of 15 cm/s. The flow was essentially linear and was quite coherent. After 10 days a marked change occurred. Buoy numbers 7161, 7168, and 7169 rapidly spread away from the other two, and a complex, incoherent flow field emerged. The flow field was analyzed by Reed and Stabeno (1990) as an example of "Lagrangian chaos". Chaotic flow results from extreme sensitivity to initial conditions where non-periodic solutions exist. No simple flow field emerges from this drifter set. One drifter (7161) moved along the slope to the northwest in agreement with our expectations of flow in the Bering Slope Current. On the other hand, buoys 7165 and 7166 eventually moved back to the southeast, and buoy 7168 had little net movement. Thus the flow field appeared to have major inhomogeneities in space and time.

An analytical criterion of chaotic flow is periods of exponential growth in line segments connecting objects (drifters). Of the ten possible line segments in the group in this first deployment, eight clearly showed periods (of 5 days' duration or longer) of exponential growth. A quantity known as the "fractal dimension" was derived and was found to be 1.2. The fact that it is not an integer probably results from not all portions of the trajectories being chaotic. The very limited number of observations elsewhere that suggest chaos show similar conditions to those here.

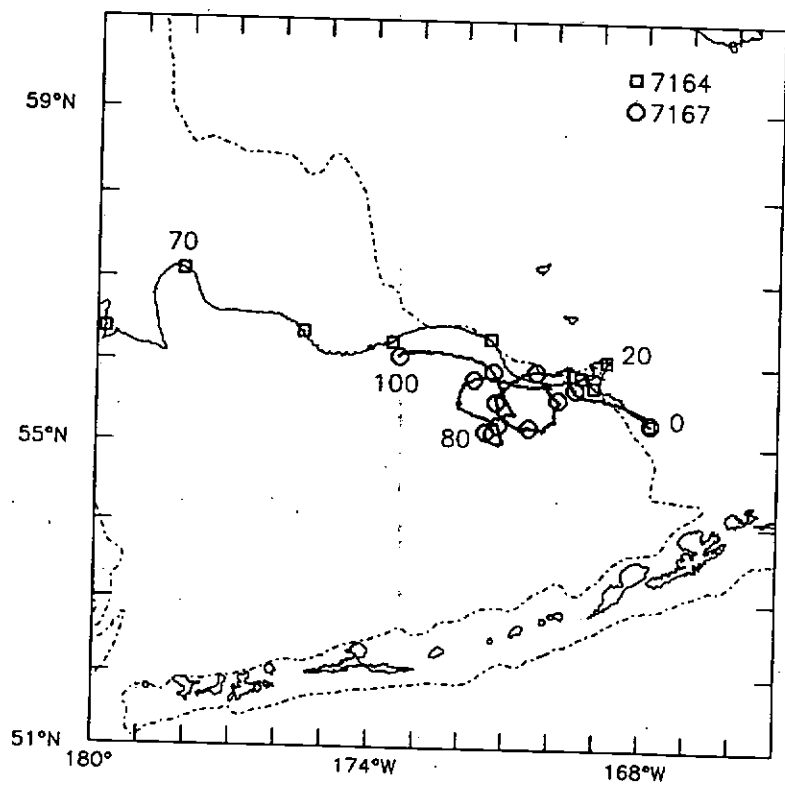
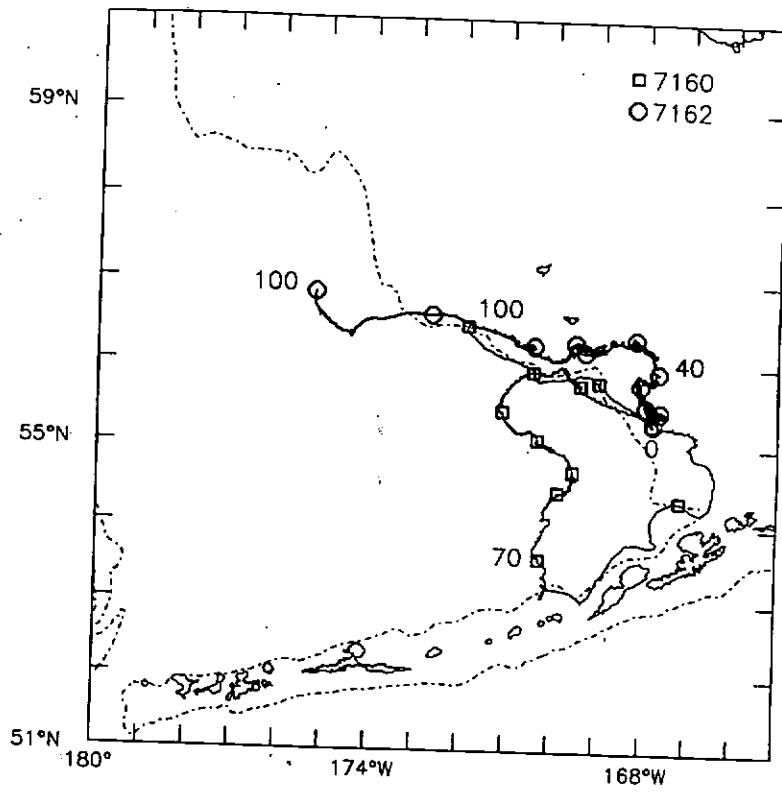
What is the relevance of the existence of Lagrangian chaos to this oceanic region? First, it implies that the low frequency flow is not very stable or persistent as indicated by the variability seen in the geostrophic flow (Fig. 3). Hence it may be difficult to adequately define circulation by traditional methods. Second, the existence of considerable high-frequency variability calls for such rapid and frequent samplings as to soon become impractical. Finally, we believe that sampling with many drifters, plus use of statistical methods, is the best solution (Stabeno and Reed, 1993). The existence of chaos in other regions of weak flow (eastern boundary currents) is apt to be prevalent.

23 September 1989 Deployment. One drifter in this set failed after two days, and its trajectory is not shown (Fig. 15). Three of these drifters moved westward, and only one (7166) looped back to the south and then moved along the slope and onto the shelf. The initial shear in the flow here was rather large, and consequently there was no convincing evidence in these data of chaotic flow. One should not conclude, however, that chaotic flow was not present but that, if so, it could not be ascertained.



Deployed: September 10, 1989

Figure 15. Trajectories of satellite-tracked drifters released on 10 September 1989. Data are shown for 100 days after release.



Deployed: September 23, 1989

Figure 16. Trajectories of satellite-tracked drifters released on 23 September 1989. Data are shown for 100 days after release.

19 April 1990 Deployment. Seven drifters were released in this set (Fig. 16). The initial flow was a weak drift toward the northwest. All of these drifters, unlike those in fall 1989, moved onto the shelf. The last half of these trajectories show a very weak, but persistent, flow toward the north. The flow field suggested by surface salinity patterns (Reed, 1991), however, was more along the isobaths.

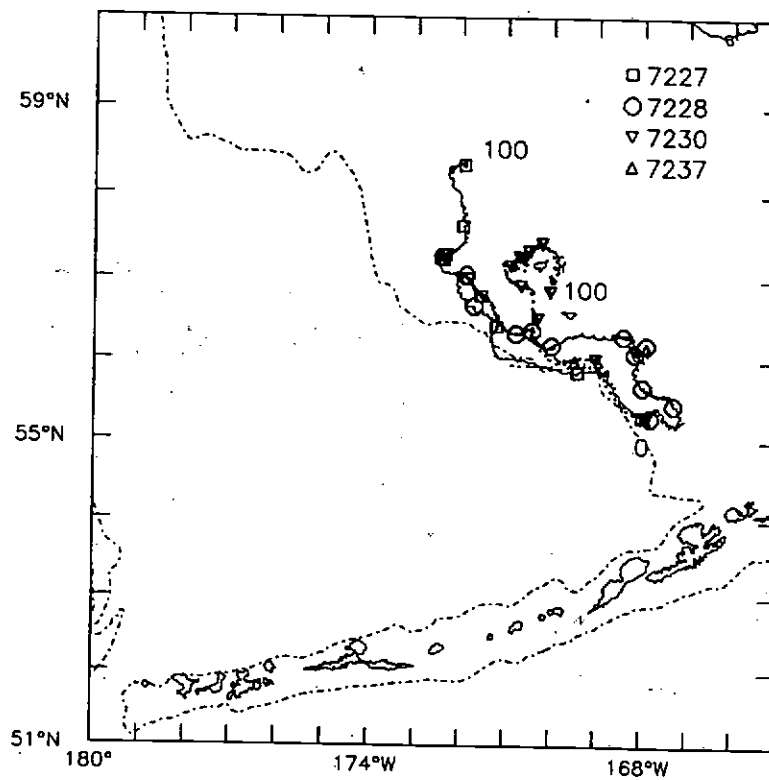
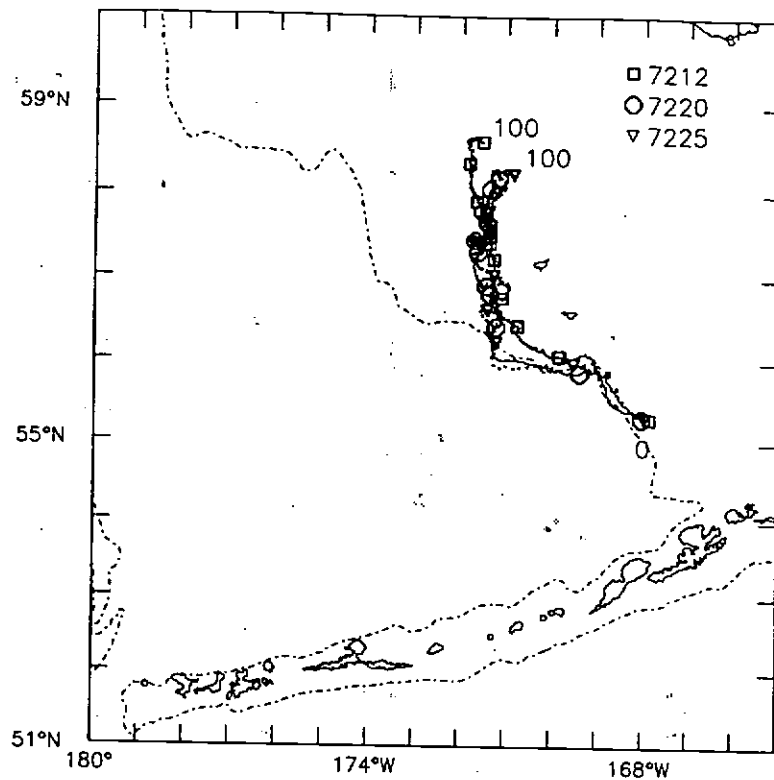
1 May 1990 Deployment. The final drifter release contained six buoys (Fig. 17). At first, flow was across the shelf toward the northeast. The initial movement of this set, and the previous one, was very similar to the geostrophic flow (Reed, 1991). Almost half of the duration of these data was spent in a small region near 55.6° N, 167.2° W. The drifters were virtually stationary there, with the only apparent force being weak horizontal diffusion. Finally a slow drift to the northwest occurred. It would be difficult to detect chaos in such weak flow because changes in position were often smaller than the standard error in the satellite-tracked drifter's position. We suspect that the weak onshore flow in spring, versus the stronger offshore movement in fall, may be a typical seasonal difference (Stabeno and Reed, 1993).

DISCUSSION

An interesting feature in the data examined here is the considerable spatial and temporal variability in the offshore (depths >1000 m) geostrophic flow, except in Pribilof and Zhemchug Canyons where it was consistently westward. (It is not clear, of course, whether the baroclinic flow is entirely "geostrophic".) Over the shelf, the flow was weak but was generally in the same direction (westward or northwestward). Except in the canyons, the offshore flow is so variable or weak that it is hard to justify identifying it as the "Bering Slope Current" (Kinder et al., 1975). Volume transport of the various branches of flow were generally $<2 \times 10^6 \text{ m}^3 \text{ s}^{-1}$, although this estimate is very crude. The flow along the slope here is presumably an eastward extension of the northward inflow through the deep pass near 180° (Sayles et al., 1979), which normally has a transport of $2\text{--}3 \times 10^6 \text{ m}^3 \text{ s}^{-1}$ (Reed, 1990). Kinder et al. (1975) concluded that much of the variability of flow along the slope was caused by planetary waves. Reed and Stabeno (1990) found a clear example of Lagrangian chaos in a set of drifter data launched at a site south of the Pribilof Islands. Three other sets of drifters launched at this site failed to show evidence of chaos. The two sets from spring 1990 showed weak net flow with suggestions of eddy diffusion.

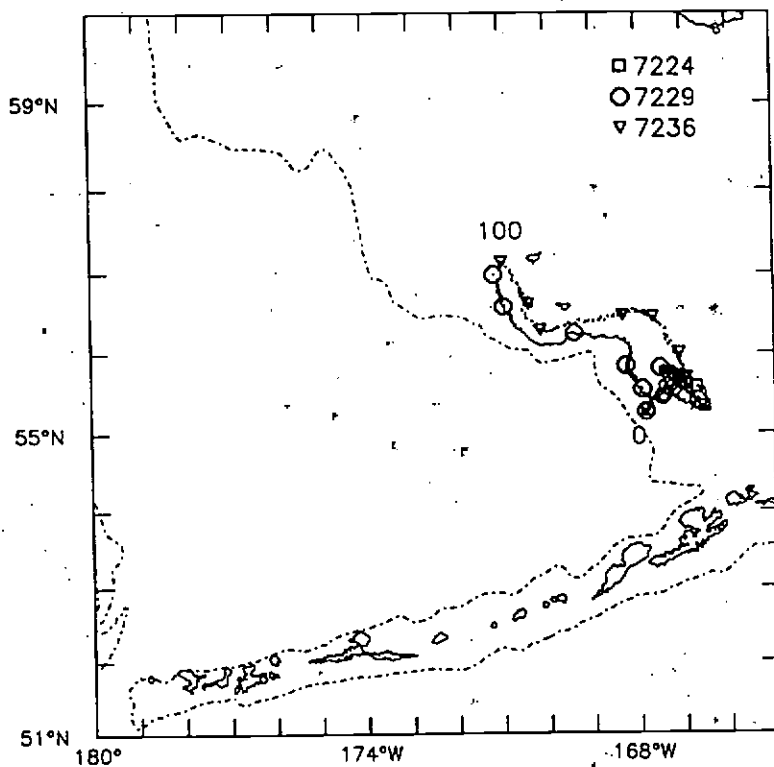
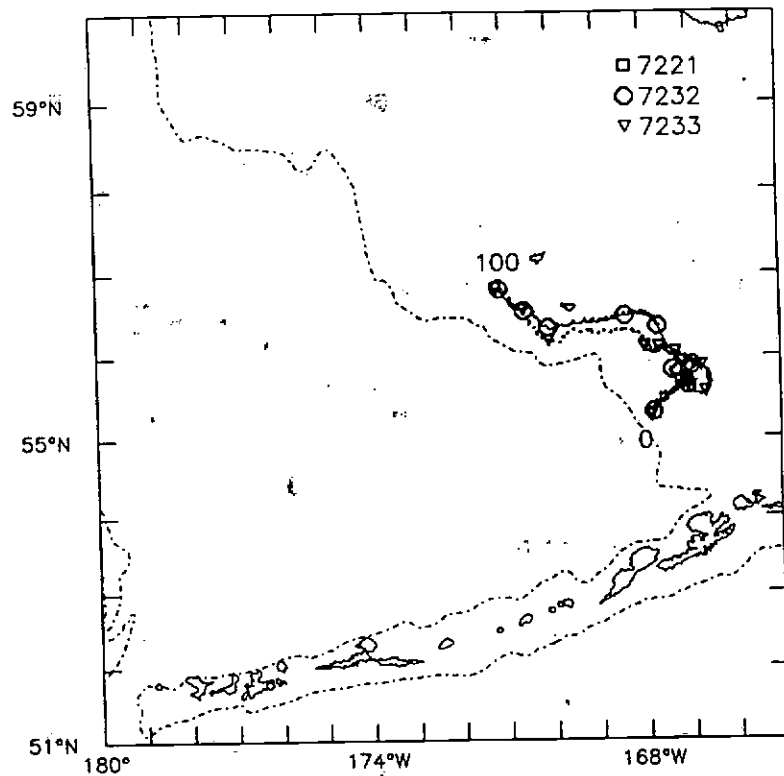
Another aspect of flow is suggested by the data in Fig. 6. During all three cruises, temperatures at $\sigma\text{-t} \sim 26.8$ were quite cold (generally $<3.7^{\circ}\text{C}$). Conversely, during fall 1986 (Reed et al., 1988) and spring 1988 (Reed and Stabeno, 1989) temperatures were $>4.0^{\circ}\text{C}$ in places. During fall 1986, at least, there was clear evidence for an inflow of warm Alaskan Stream water through Amukta Pass (near 172°W) that produced the warm subsurface water. Relatively cold temperatures during the three cruises reported here, during August 1972 (Kinder et al., 1975), and during June 1987 (Reed et al., 1988), however, suggest the absence of inflow, or at least a weak inflow, through Amukta Pass. The temperature of Alaskan Stream source waters seem not to vary greatly; thus there appears to be appreciable variability in the inflow as well as variability in flow all along the slope.

The current records show a northwestward flow which follows the bathymetry of the continental slope in the eastern Bering Sea. This flow primarily occurred in the upper 300 m of the water column and generally did not respond to the marked winter-time increase in wind stress. These results suggest that the observed flow was part of the basin-scale circulation that is modified by topography, integrating the seasonal wind signal (as in the Alaskan Stream: Cummins, 1989). The strength of the flow was weaker near Zhemchug Canyon than at the two other array sites. This suggests that the majority of the transport flows west over the basin rather than flowing northwestward past Zhemchug Canyon. This flow pattern is consistent with



Deployed: April 19, 1990

Figure 17. Trajectories of satellite-tracked drifters release on 19 April 1990. Data are shown for 100 days after release.



Deployed: May 1, 1990

Figure 18. Trajectories of satellite-tracked drifters released on 1 May 1990. Data are shown for 100 days after release.

previous results from dynamic topography (e.g., Kinder et al., 1975) and satellite-tracked buoy trajectories launched in September 1989 and April–May 1990.

Is this flow the Bering Slope Current? The observed currents do not support the concept of alternating bands of flow (Kinder et al., 1975). However, there were no direct current measurements seaward of the 1000 m isobath. Further, the presence of eddies complicates interpretation of geopotential topography: inferred cross-slope flow may sometimes be a result of large along-slope separation of CTD lines with an eddy located near one of the lines. The dynamic topography presented here does indicate regions of both northwest and southeast flow. Using the records from BS3 and BS2, we can estimate mean transport. The calculation is based on the assumption that speeds observed at BS3 represented flow from about 3 km seaward of the mooring to the midpoint between BS3 and BS2, and speeds at BS2 extended shelfward for about 1 km. The estimated mean transport was $\sim 2 \times 10^6 \text{ m}^3/\text{s}$, or about half that suggested previously for the Bering Slope Current (Kinder et al., 1975). Considering their results in finer detail (Kinder et al., 1975, Fig. 15), about $2 \times 10^6 \text{ m}^3/\text{s}$ flow toward the northwest in the vicinity of the BS moorings. It is possible that our observations mainly represent flow in the shoreward segment of the Bering Slope Current.

The strong bottom currents at BP2 were not accounted for by correlation with the wind. Their period (14 d) suggests that interaction between tidal currents and canyon bathymetry could be the forcing mechanism. A record segment from BP2 (272 m) shows a marked similarity between tidal current amplitude and the low frequency (subtidal) flow (Fig. 14). During spring tides, low frequency current speeds approached 20 cm/s, whereas during neap tides there were weak reversals in flow. The hourly current record from 272 m was demodulated to create daily and semidaily constituent time series, and estimates of correlation were calculated between these two new series and the three low-pass filtered series. The results showed significant (99% level) correlation between the demodulated series of daily frequency and the low-pass series (0.52, 0.43, and 0.36 at 272, 137 and 62 m respectively). The only significant correlations between demodulated semidaily and low-pass time series was at 272 m (0.30). As expected from the relative strength of the tidal constituents (Table 1A), most of the low frequency fluctuations were accounted for by the demodulated K1 tidal current. Furthermore, the rectified bottom tidal current resulted in fluctuations throughout the water; these decreased with increasing height above the bottom, however.

Some of the current fluctuations were due to the passage of eddies. There were four current reversals which persisted for more than 5 days at BS3 (45 m). The most pronounced occurred between 16 and 27 May 1990. During this event, flow also reversed at BS2. Water property data from BS3 indicated that temperature at 45 and 120 m depths increased by 0.5°C and 0.3°C , respectively. Simultaneously, salinity at 120 m decreased by approximately -0.2 ‰ . These changes suggest the presence of a clockwise rotating eddy. The mean along-slope speed during the passage of the eddy was 28 cm/s (at 45 m) decreasing to 15 cm/s at 495 m. Using estimates of translation speeds for eddies in the Bering Sea of 0.5 cm/s (Kinder et al., 1980) or 1–2 cm/s (Reed and Stabeno, 1988), the radius of the present feature was between 5 and 20 km.

Eddies have been identified in prior studies from drogued trajectories, hydrographic data, and satellite images (Paluszkiwicz and Niebauer, 1984: their Table 1). Typically, however, these features have diameters $>100 \text{ km}$. The observed rotational speed and estimate of size for the present eddy is in agreement with small (5–10 km radius) eddies more recently identified using satellite tracked buoys (drogued at 40 m) over an adjacent region of the eastern Bering slope (Reed and Stabeno, 1988). It appears that station separation used in hydrographic surveys has under sampled small eddies. Such eddies, however, appear to be common and are an important feature over the outer continental shelf and slope.

Considerable variability exists in the drifter paths. At times, Lagrangian chaos appears to be a major factor in the evolution of the flow field. These and other data are perhaps suggestive of a seasonal change in flow. In fall-winter a relatively strong westward flow across the eastern and central basin seems typical; in spring-summer of 1990, at least, much weaker flow, mainly across the shelf, was present.

ACKNOWLEDGEMENTS

We especially thank Carol DeWitt for her many efforts and for serving as Chief Scientist on two of these cruises. The efforts of the officers and crew of the NOAA ship *Miller Freeman* are also appreciated. S. Bograd, K. Kroglund, D. Lambourn, L. Lawrence, L. Long, W. Parker, and P. Proctor assisted with data collection, preparation, and analysis. We also thank Phyllis Stabeno for enthusiastic discussions and assistance and Jaweed Hameedi for his many efforts. This work was supported by the Outer Continental Shelf Environmental Assessment Program of NOAA and the Minerals Management Service of the Department of the Interior.

REFERENCES

- Coachman, L. K. 1986. Circulation, water masses, and fluxes on the southeastern Bering Sea shelf. *Cont. Shelf Res.* 5:23-108.
- Cummins, P. F. 1989. A quasi-geostrophic circulation model of the northeast Pacific: Part II: Effects of topography and seasonal forcing. *J. Phys. Oceanogr.* 19:1649-1668.
- Fischer, J. M., P. R. Carlson, and H. A. Karl. 1982. Bathymetric map of Navarin basin providence, northern Bering Sea. U.S. Geol. Surv., Open-File Rep., 82-1038. 11 pp.
- Hansell, D. A., J. J. Goering, J. J. Walsh, C. P. McRoy, L. K. Coachman, and T. E. Whitledge. 1989. Summer phytoplankton production and transport along the shelf break in the Bering Sea. *Cont. Shelf Res.* 9:1085-1104.
- Hughes, F. W., L. K. Coachman, and K. Aagaard. 1974. Circulation, transport and water exchange in the western Bering Sea. Pp. 59-90 in *Oceanography of the Bering Sea, with Emphasis on Renewable Resources*. Institute of Marine Science, University of Alaska, Fairbanks.
- Karl, H. A., and P. R. Carlson. 1987. Surface current patterns suggested by suspended sediment distributions over the outer continental margin, Bering Sea. *Mar. Geol.* 74:301-308.
- Kinder T. H. 1976. The continental slope regime of the eastern Bering Sea. Ph.D. thesis, University of Washington, Seattle.
- Kinder, T. H., L. K. Coachman, and J. A. Galt. 1975. The Bering Slope current system. *J. Phys. Oceanogr.* 5:231-244.
- Kinder, T. H., and L. K. Coachman. 1978. The front overlying the continental slope in the eastern Bering Sea. *J. Geophys. Res.* 83:4551-4560.
- Kinder, T. H., J. D. Schumacher, and D. V. Hansen. 1980. Observation of a baroclinic eddy: an example of mesoscale variability in the Bering Sea. *J. Phys. Oceanogr.* 10:1228-1245.
- Kinder, T. H., D. C. Chapman, and J. A. Whithead, Jr. 1986. Westward intensification of the mean circulation on the Bering Sea shelf. *J. Phys. Oceanogr.* 16:1217-1229.
- Mofjeld, H. O. 1986. Observed tides on the northeastern Bering Sea Shelf. *J. Geophys. Res.* 91:2593-2606.
- Muench, R. D., and J. D. Schumacher. 1985. On the Bering Sea ice edge front. *J. Geophys. Res.* 90:3185-3197.
- Paluszkiwicz, T., and H. J. Niebauer. 1984. Satellite observations of circulation in the eastern Bering Sea. *J. Geophys. Res.* 89:3663-3678.
- Parsons, T. R., Y. Maita, and C. M. Lalli. 1984. *A Manual of Chemical and Biological Methods for Seawater Analysis*. Pergamon Press, Oxford. 173 pp.
- Pearson, C. A., H. O. Mofjeld, and R. B. Tripp. 1981. Tides of the Eastern Bering Sea Shelf. Pp. 111-130 in *The Eastern Bering Sea Shelf: Oceanography and Resources*, vol. 1. U.S. Government Printing Office, Washington D.C.
- Reed, R. K. 1990. A year-long observation of water exchange between the North Pacific and the Bering Sea. *Limnol. Oceanogr.* 35:1604-1609.
- Reed, R. K. 1991. Circulation and water properties in the central Bering Sea during OCSEAP studies, fall 1989-fall 1990. NOAA Tech. Rep. ERL 446-PMEL 41, NOAA Environmental Research Laboratories, Boulder, CO. 14 pp.
- Reed, R. K., and J. D. Schumacher. 1986. Current measurements along the shelf break in the Gulf of Alaska. *J. Phys. Oceanogr.* 16:1985-1990.
- Reed, R. K., and P. J. Stabeno. 1989. Circulation and property distributions in the central Bering Sea, spring 1988. NOAA Tech. Rep. ERL 439-PMEL 39, NOAA Environmental Research Laboratories, Boulder, CO. 13 pp.
- Reed, R. K., and P. J. Stabeno. 1990. Flow trajectories in the Bering Sea: Evidence for chaos. *Geophys. Res. Lett.* 17:2141-2144.
- Reed, R. K., J. D. Schumacher, and A. T. Roach. 1988. Geostrophic flow in the central Bering Sea, fall 1986 and summer 1987. NOAA Tech. Rep. ERL 433-PMEL 38, NOAA Environmental Research Laboratories, Boulder, CO. 13 pp.

- Sayles, M. A., K. Aagaard, and L. K. Coachman. 1979. Oceanographic atlas of the Bering Sea Basin. University of Washington Press, Seattle. 158 pp.
- Schumacher, J. D., and T. H. Kinder. 1983. Low-frequency current regimes over the Bering Sea shelf. *J. Phys. Oceanogr.* 13:607-623.
- Schumacher, J. D., and R. K. Reed. 1992. Characteristics of currents over the continental slope of the eastern Bering Sea. *J. Geophys. Res.* 97:9423-9433.
- Schumacher, J. D., R. K. Reed, and P. J. Stabeno. 1992. Circulation and fluxes near the eastern Bering Sea continental slope. Pp. 53-64 in Fourth Information Transfer Meeting, Conference Proceedings, OCS Study MMS 92-0046, Minerals Management Service, Anchorage, Alaska.
- Stabeno, P. J., and R. K. Reed. 1993. Circulation in the Bering Sea basin observed by satellite-tracked drifters: 1986-1992. *J. Phys. Oceanogr.* (submitted).
- Whitledge, T., S. Malloy, C. Patton, and C. Wirick. 1981. Automated nutrient analyses in seawater. BNL Rep. 51398, Brookhaven National Laboratory, Upton, NY. 216 pp.
- Whitledge, T. E., W. S. Reeburgh, and J. J. Walsh. 1986. Seasonal inorganic nitrogen distributions and dynamics in the southeastern Bering Sea. *Cont. Shelf Res.* 5:109-132.

LIST OF TABLES

Table 1. Mooring locations, observation period, and mean current.

Table 2. Kinetic energy in winter (89274–90090) and summer (90152–90243). The units are cm^2/s^2 for the currents and m^2/s^2 for the winds, and both are per unit mass.

Table 3. Fluxes of momentum ($\overline{u'v'}$, $\text{cm}^2 \text{s}^{-2}$), heat ($\overline{u'T'}$ and $\overline{v'T'}$, $\text{cm } ^\circ\text{C s}^{-1}$), and salt ($\overline{u'S'}$ and $\overline{v'S'}$, $\text{cm } \text{‰} \text{s}^{-1}$) at the current moorings. The standard error (based on the variance and the integral time scale) is also given. v is in the direction of maximum variance (generally "along-stream"), and u is 90° to the right of v .

Table 1A. Result of 29-day harmonic analysis of current records in ellipse representation. Start time for the analysis of records from the slope was JD335, 1989; all other analyses began on JD130, 1990.

TABLE 1. Mooring Locations, Observation Period and Mean Current.

Location, mooring name, and water depth (N. Lat., W. Long., m)	Instrument Depth (m)	Observation Period (JD)	Mean speed \pm RMS ¹ error, direction (cm s ⁻¹ , °T)	Axis of greatest variance and % total variance (°T, %)
<i>Pribilof Canyon</i>				
BP3: slope 56.12, 169.27 1002 m	52	89256-90131	5.6 \pm 2.0, 277	296, 62%
	127	89256-90116	4.5 \pm 1.4, 246	279, 52%
	262	89256-90109	1.7 \pm 0.8, 246	142, 54%
	502	89256-90258	2.5 \pm 0.8, 126	121, 85%
BP2A: mid-slope 56.16, 168.88 275 m	49	90111-90245	10.3 \pm 2.6, 266	272, 78%
	124	90111-90245	7.4 \pm 2.6, 267	269, 89%
	260	90123-90244	7.5 \pm 2.0, 247	258, 92%
BP2: mid-slope 56.23, 169.70 287 m	62	89256-90250	6.0 \pm 1.8, 228	214, 81%
	137	89256-90250	3.9 \pm 1.6, 237	206, 90%
	272	89256-90250	10.8 \pm 1.2, 189	190, 82%
BP1: outer shelf 56.27, 169.80 140 m	50	90112-90279	6.7 \pm 1.8, 240	223, 80%
	125	90112-90279	5.8 \pm 2.8, 200	208, 91%
<i>Central Slope</i>				
BS3: slope 56.67, 173.29 995 m	45	89257-90277	17.9 \pm 6.0, 311	311, 93%
	120	89257-90251	11.2 \pm 5.0, 301	301, 95%
	255	89257-90187	5.9 \pm 4.6, 309	304, 96%
	495	89257-90277	1.4 \pm 1.8, 315	301, 97%
BS2: mid-slope 56.69, 173.25 274 m	49	90112-90276	16.1 \pm 3.7, 311	310, 85%
	125	90112-90276	16.0 \pm 3.8, 311	311, 92%
	260	90112-90276	11.2 \pm 3.6, 318	313, 99%

Zhemchug Canyon

BZ3: slope	48	89259-90125	3.0 ± 1.2, 288	228, 58%
58.55, 175.05	123	89259-90123	2.0 ± 1.4, 289	232, 61%
998 m	258	89259-90274	1.9 ± 1.6, 256	221, 68%
	498	89259-90274	0.9 ± 1.0, 234	233, 70%
BZ2: mid-slope	46	90114-90273	4.3 ± 1.2, 258	246, 75%
58.64, 175.12	121	90114-90273	5.2 ± 1.4, 240	241, 87%
271 m	260	90114-90273	1.8 ± 0.8, 230	219, 91%

¹ where $RMS = 2 \times [\text{variance} \times \text{integral time scale}/\text{record length}]^{1/2}$

TABLE 2. Kinetic energy in winter (89274-90090) and summer (90152-90243). The units are cm^2/s^2 for the currents and m^2/s^2 for winds, and both are per unit mass.

Nominal depth (m)	<u>BP3</u> W/S	<u>BP2</u> W/S	<u>BP2A</u> W/S	<u>BP1</u> W/S	<u>WIND</u> W/S
50	43/-	38/28	-/24	-/23	47/20
125	26/-	60/10	-/25	-/47	
260	10/-	19/16	-/29		
500	15/7				
	<u>BS3</u> W/S	<u>BS2</u> W/S			
50	145/102	-/54			53/23
125	98/37	-/45			
260	68/-	-/40			
500	26/12				
	<u>BZ3</u> W/S	<u>BZ2</u> W/S			
50	22/-	-/9			46/23
125	41/-	-/10			
260	30/7	-/6			
500	9/2				

TABLE 3. Fluxes of momentum ($\overline{u'v'}$, $\text{cm}^2 \text{s}^{-2}$), heat ($\overline{u'T'}$ and $\overline{v'T'}$, $\text{cm} \text{ }^\circ\text{C s}^{-1}$), and salt ($\overline{u'S'}$ and $\overline{v'S'}$, $\text{cm } \text{‰ s}^{-1}$) at the current moorings. The standard error (based on the variance and the integral time scale) is also given. v is in the direction of minimum variance (generally "alongstream"), and u is 90° to the right of v .

Mooring	Depth (m)	Dir. of max. var. ($^\circ$)	$\overline{u'v'}$	$\overline{u'T'}$	$\overline{u'S'}$	$\overline{v'T'}$	$\overline{v'S'}$
BP3	52	290	1.0±4.2	-0.2±1.0	0.3±0.6	1.2±0.7	0.5±0.4
	127		-0.5±2.4	0.5±0.4	0.1±0.1	0.2±0.4	0.1±0.1
	262		0.6±1.2	0.1±0.1	0.0±0.0	-0.1±0.1	0.0±0.0
	502		2.3±0.7	0.0±0.0	0.0±0.0	0.0±0.0	0.0±0.0
BP2A	49	265	4.1±4.0	0.7±1.1	0.3±0.2	-0.4±0.4	0.1±0.1
	124		2.6±1.9	0.1±0.2	0.1±0.1	-0.1±0.1	0.0±0.0
	260		-3.7±2.2	0.1±0.1	0.1±0.0	0.0±0.0	0.0±0.0
BP2	62	210	3.1±1.9	0.9±1.0	1.3±0.6	-0.3±0.3	0.0±0.0
	137		-3.4±2.2	0.2±0.5	0.3±0.8	-0.1±0.1	-0.2±0.1
	272		-7.7±1.2	-0.2±0.1	-0.8±0.4	0.0±0.0	-0.2±0.1
BP1	50	210	5.4±2.3	3.1±1.1	0.2±0.1	0.6±0.5	0.0±0.1
	125		-1.9±3.1	0.2±0.2	0.3±0.2	0.0±0.1	0.1±0.0
BS3	45	310	3.6±7.5	-0.6±0.7	2.2±1.4	0.0±0.2	0.1±0.3
	120		-28.4±6.0	0.1±0.4	0.5±0.1	0.0±0.1	-0.1±0.0
	255		-13.6±3.6	0.1±0.2	0.2±0.1	0.0±0.0	0.0±0.0
	495		-6.9±1.3	0.0±0.0	0.0±0.0	0.0±0.0	0.0±0.0
BS2	49	310	-0.6±6.5	2.0±3.8	0.3±0.3	-1.7±1.0	0.1±0.1
	125		2.9±4.0	-0.5±1.0	0.6±0.3	-0.2±0.2	0.0±0.0
	260		9.1±3.1	0.3±0.2	0.5±0.3	0.0±0.0	0.0±0.0
BZ3	48	230	0.4±2.8	0.7±0.9	0.0±0.1	-1.8±0.9	0.0±0.1
	123		-0.1±3.4	0.2±1.2	0.0±0.1	0.5±0.4	0.0±0.1
	258		-2.4±1.8	0.0±0.1	0.0±0.0	0.1±0.1	0.0±0.0
	498		0.3±0.5	0.0±0.0	0.1±0.0	0.0±0.0	0.0±0.0
BZ2	46	240	0.9±0.7	-1.2±0.8	0.1±0.1	0.0±0.0	0.0±0.0
	121		0.0±0.1	-0.1±0.3	0.0±0.0	0.1±0.1	0.0±0.0
	260		-2.3±0.5	0.0±0.1	0.0±0.0	0.0±0.0	0.0±0.0

APPENDIX I

Publications Resulting from This Data Set:

1. Reed, R. K., and P. J. Stabeno. 1990. Flow trajectories in the Bering Sea: Evidence for chaos. *Geophys. Res. Lett.* 17:2141-2144.
2. Reed, R. K. 1991. Circulation and water properties in the central Bering Sea during OCSEAP studies, fall 1989-fall 1990. NOAA Tech. Rep. ERL 446-PMEL 41, NOAA Environmental Research Laboratories, Boulder, CO. 14 pp.
3. Schumacher, J. D., and R. K. Reed. 1992. Characteristics of currents over the continental slope of the eastern Bering Sea. *J. Geophys. Res.* 97:9423-9433.
4. Schumacher, J. D., R. K. Reed, and P. J. Stabeno. 1992. Circulation and fluxes near the eastern Bering Sea continental slope. Pp. 53-64 in *Fourth Information Transfer Meeting, Conference Proceedings, OCS Study MMS 92-0046, Minerals Management Service, Anchorage, Alaska.*

APPENDIX II

We present characteristics of the major tidal current constituents (Table 1A) in a format like Pearson et al. (1981) so that co-amplitude and co-phase maps can be extended to the slope. Tidal energy over the basin mainly propagates in from the Pacific Ocean; the minor contribution from the Arctic Ocean influences tides only over the northeastern portion of the continental shelf (Pearson et al., 1981; Mofjeld, 1986). In most areas of the eastern Bering Sea the tide is the mixed semidiurnal type (Pearson et al., 1981), however, results from more recent observations suggest that the diurnal tides dominate (Mofjeld, 1986) over the northeastern portion of the shelf. Tidal harmonic constants fluctuate seasonally over much of this shelf; this may be a response to changes in ice cover (Pearson et al., 1981; Mofjeld, 1986). Because of this behavior, we have selected two 29 d segments on the basis of the amplitudes of the constituents being close to the mean amplitude for all consecutive 29 d segments, and that these segments include portions of all the current records.

TABLE 1A. Result of 29-day harmonic analyses of current records in ellipse representation¹. Start time for the analyses of records from the slope was JD 335, 1989; all other analyses began on JD130, 1990.

Record/Depth (m)	SLOPE																			
	H	G	D _{O₁}	H	R	H	G	D _{K₁}	H	R	H	G	D _{N₂}	H	R	H	G	D _{M₂}	H	R
BZ3																				
48 m	2.2	130	261	0.8	C	2.8	160	258	1.5	C	3.5	105	55	3.0	C	8.7	121	358	8.3	C
123 m	2.3	94	237	0.6	C	3.5	153	237	2.3	C	3.1	24	347	2.5	C	8.7	110	359	7.2	C
258 m	1.8	106	236	0.4	C	2.7	166	249	1.3	C	2.1	13	14	1.5	C	5.4	95	37	4.1	C
498 m	1.6	90	227	0.1	C	1.9	133	198	1.6	C	2.0	216	327	1.8	C	5.7	44	106	3.4	C
BS3																				
45 m	0.8	163	323	0.3	C	1.9	243	191	0.3	C	3.1	95	324	1.5	C	5.5	125	123	3.8	C
120 m	0.6	235	353	0.3	C	1.3	238	180	0.3	AC	3.3	99	350	1.4	C	5.2	132	148	3.3	C
255 m	1.9	96	302	0.0	C	1.9	126	143	0.2	AC	1.5	140	292	1.1	C	1.8	101	203	0.4	C
495 m	0.9	127	297	0.0	AC	1.1	116	130	0.1	C	1.4	18	280	1.1	C	1.6	49	295	0.8	C
BP3																				
52 m	2.8	46	237	0.1	C	4.6	73	240	1.7	C	2.8	77	10	2.0	C	5.6	163	354	3.1	C
127 m	1.6	74	203	0.1	C	3.4	106	211	0.6	C	3.4	24	4	2.9	C	7.6	86	351	5.9	C
262 m	1.2	253	188	0.7	AC	2.3	31	287	2.0	C	4.2	12	23	3.7	C	12.2	87	16	10.4	C
502 m	3.7	155	106	0.3	C	7.7	14	299	0.5	C	1.8	175	20	1.5	C	7.5	210	312	5.9	C
BZ2																				
46 m	5.0	157	273	2.7	C	7.0	159	272	4.4	C	1.3	77	26	1.1	C	7.9	163	28	6.5	C
121 m	5.2	142	252	2.3	C	8.4	169	261	5.0	C	2.9	152	50	2.1	C	7.2	154	347	5.6	C
260 m	4.1	152	228	1.4	C	4.8	176	235	1.9	C	1.2	117	339	0.4	C	3.4	3	4	3.1	C

MID-SLOPE

MID-SLOPE

		BS2																			
	49 m	1.9	192	174	1.3	C	2.7	233	184	2.3	C	2.5	133	333	1.7	C	14.0	166	312	13.1	C
	125 m	1.7	191	174	1.4	C	2.7	227	178	2.2	C	1.4	2	312	1.1	C	10.3	183	318	8.8	C
	260 m	1.6	80	166	0.6	C	1.5	265	226	1.3	C	1.4	247	352	0.0	C	4.7	195	358	3.5	C
		BP2A																			
	49 m	5.9	147	269	2.8	C	7.9	170	269	3.5	C	6.0	83	36	3.0	C	19.1	141	29	13.9	C
	124 m	5.1	163	278	0.9	C	6.8	173	272	2.6	C	4.4	92	55	2.1	C	11.1	138	52	7.1	C
	260 m	5.3	102	268	2.8	C	6.7	75	253	4.1	C	2.4	196	44	1.7	C	10.5	100	107	9.1	C
		BP2																			
	62 m	2.6	157	201	0.6	C	4.6	39	167	1.1	C	3.8	88	38	2.4	C	12.7	154	36	10.6	C
	137 m	5.1	144	191	0.5	C	10.8	19	155	5.8	C	2.1	16	43	1.3	C	5.8	74	10	9.8	C
	272 m	8.0	155	133	0.1	C	19.8	40	137	4.7	C	2.7	123	143	0.7	C	6.5	103	122	4.5	C
		OUTER SHELF																			
		OUTER SHELF																			
		BP1																			
	50 m	3.9	33	16	0.8	C	8.5	47	176	3.4	C	4.4	123	57	3.1	C	9.0	159	43	6.5	C
	125 m	6.0	10	.9	0.7	C	15.7	60	168	2.9	C	4.2	114	116	4.2	C	12.0	179	108	9.3	C

¹ Amplitudes H are cm/s, phases G are referred to Greenwich, and direction D of the major axis is in °T. C refers to clockwise rotation and A to anticlockwise rotation.